

Magnetically driven microrobots: Recent progress and future development



Honglin Shen^a, Shuxiang Cai^a, Zhen Wang^a, Zhixing Ge^b, Wenguang Yang^a

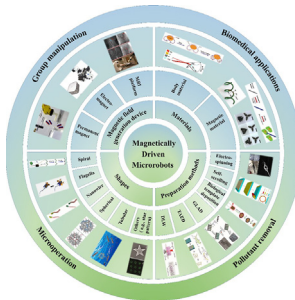
^a School of Electromechanical and Automotive Engineering, Yantai University, Yantai 264005, China

^b State Key Laboratory of Robotics, Shenyang Institute of Automation, Chinese Academy of Sciences, Shenyang 110016, China

HIGHLIGHTS

- Construction and driving method of magnetic field and materials and shapes of magnetically driven microrobots are reviewed.
- Manufacturing method and applications of magnetically driven microrobot are reviewed.
- The challenges and future directions of magnetically driven microrobot for biomedical applications are summarized.

GRAPHICAL ABSTRACT



ARTICLE INFO

Article history:

Received 19 May 2022

Revised 8 January 2023

Accepted 11 February 2023

Available online 13 February 2023

Keywords:

Magnetic-driven microrobots

Magnetic field

Manufacturing method

Biological application

ABSTRACT

Microrobots have received extensive attention in the past few decades, and the in-depth research of micro-nano processing technology and micro-nano materials has promoted the further development of microrobots. Researchers have successfully achieved the use of chemical fuels, and electric, sound, and magnetic fields to promote the movement of microrobots. Among many power sources, magnetic fields have attracted wide attention because of their advantages including remote wireless operation and harmlessness to the human body. After decades of development, magnetically driven microrobots have been extensively studied in the fields of cargo transportation, cell manipulation, toxic substance removal, and micromanipulation. This article first summarizes the driving methods of magnetically driven microrobots in recent years, then summarizes the materials for manufacturing microrobots, and summarizes the shapes of typical microrobots, including spiral, spherical, and linear structures. After that, the processing methods are sorted out, and the application of magnetic-driven microrobots in biomedicine and other fields in recent years is summarized. Finally, the development prospects of magnetic-driven microrobots are discussed.

© 2023 The Author(s). Published by Elsevier Ltd. This is an open access article under the CC BY-NC-ND license (<http://creativecommons.org/licenses/by-nc-nd/4.0/>).

1. Introduction

In 1959, the first industrial robot, Unimate, was created by American inventor Ingerberg and others. After more than half a century of development, the research of robots has experienced three stages of development, respectively for program control robots, adaptive robots, and intelligent robots. With the increase

in the demand for small-scale space operations [1–3], the operation of the traditional methods has been unable to meet demand. Due to the development of micro-nano processing technology and further research into micro-nano materials. Scientists divide robots into nanorobots (on the nanoscale), microrobots (size on the micron scale), millirobots (size on the millimeter scale), and robots (size on the meter scale) based on their size, in this review we consider that microrobot covers the nanorobot, microrobot, and millirobot. It is considered to have broad prospects in the fields of

E-mail addresses: gezhixing@sia.cn (Z. Ge), ytu_yangwg@163.com (W. Yang)

cargo transportation [4–6], minimally invasive surgery [7–9], micromanipulation [10], and removal of toxic and harmful substances [11–13], the research of microrobot has attracted extensive attention of researchers. The development of the microrobot has successfully built a bridge between the robot and micro field, broadened the application field of the robot, realized the span of mechanical and electrical products from the macro field to the micro field, and promoted the development of mechatronics integration.

Through the research on the driving and control strategy of the microrobots, it is found that the microrobots cannot carry the traditional battery energy. The energy supply for microrobots can be roughly divided into chemical drive, physical drive, or a combination of chemical drive and physical drive. The chemical driving method generally converts chemical energy into kinetic energy through a chemical reaction. A common chemical driving method is to decompose hydrogen peroxide (H_2O_2) to produce bubbles to achieve driving [14–16]. However, H_2O_2 is considered to be a harmful substance to the human body, so it is difficult to be further used in the human body. The physical driving method mainly uses electric field [17,18], magnetic field [19–23], light field [24–26], and sound field [27–29] as the power source. Among the various methods, the magnetic field has the advantages of high controllability, no pollution, and the ability to penetrate biological tissues. Therefore, the magnetic field has been widely used to drive microrobots. When microrobots are used in humans, the first consideration is that they are harmless to humans. The researchers chose biocompatible materials [30–32] to make the microrobot, which can degrade the body after completing the task, so as not to cause harm to the human body. In addition, when the magnetic part of the microrobot needs to be removed, the researchers use an external magnetic field to recover the magnetic material [33–35], so that the magnetic material can be removed from the body after the completion of the task.

When a magnetically driven microrobot moves in a liquid environment and macroscopic driving methods are no longer applicable in the microscopic field. New driving theories need to be studied for efficient driving research of microrobots. In a liquid environment with a low Reynolds number, the viscosity of the liquid can quickly eliminate the influence of inertia. The main effect is no longer the inertial force, but the viscous force [36]. Microrobots are generally in a low Reynolds number environment because of their small size. In the incompressible Newtonian liquid with a low Reynolds number, the microrobot must break the reversibility of deformation in time to generate a net displacement and achieve forward advancement [37]. The efficient movement of microorganisms in a fluid environment with a low Reynolds number provides scientists with ideas. One type is Escherichia coli, algae, and other spiral flagella that rotate by themselves [31,38], which converts rotational movement into translational movement. The other is the fluctuating movement of the sperm flagella [39,40], which realizes its forward propulsion. Researchers have studied the above-mentioned biological structure and manufactured artificial and biological hybrid microrobots according to the different manufacturing materials. Various shapes and structures of microrobots will be introduced in detail in later sections. In addition to studying the control of individual robots, the control of groups has also attracted the attention of researchers [41,42]. At the same time, except for the group control of microrobots, how to selectively manipulate a single microrobot in swarm control is also an important direction [43–45].

After decades of development, microrobots have made extensive achievements [46–51]. In summary, as shown in Fig. 1, the development of magnetically driven microrobots in recent years was reviewed. First, we summarize the construction and drive theory of magnetic fields, and then introduce the shape of

microrobots. On this basis, we summarize the manufacturing materials and manufacturing methods of microrobots. After that, a series of applications of microrobots are introduced, and finally, the future development direction of magnetic-driven microrobots is analyzed.

2. Magnetic drive system

According to the force characteristics of the microrobots in the magnetic field, the driving mode can be divided into magnetic force drive and magnetic torque drive. The magnetic force F and magnetic torque T can be obtained as follows:

$$F = V(\mathbf{M} \cdot \nabla)\mathbf{B} \quad (1)$$

$$\mathbf{T} = VM \times \mathbf{B} \quad (2)$$

where \mathbf{B} is the magnetic flux density and \mathbf{M} is the magnetic moment of the magnet, V is the volume of the magnetic object.

For magnetic force drive, the gradient of a magnetic field can be used to drive a microrobot if it can overcome viscous resistance forces. For magnetic torque drive, when the direction of the applied magnetic field is different from that of the magnetic dipole moment, the magnetic dipole moment of the microrobot is reflected in the direction of the magnetic field until it overlaps. The motion control of the microrobot is realized by changing the direction of the magnetic field constantly. At present, two methods have been mainly studied for the generation of magnetic fields to control microrobots. They are driven by permanent magnets and electromagnets. Electromagnets include air core type and iron core type, Maxwell coils and Helmholtz coils are typical examples of air core type. The OctoMag system developed by Nelson's team is the epitome of the iron core type [52]. To expand the volume of the workspace for human research, medical imaging platforms such as magnetic resonance imaging are currently used. The platform has been used to drive microrobots. Table 1 summarizes the actuation methods and their advantages and disadvantages.

2.1. Permanent magnet actuators

Compared with electromagnets, permanent magnets do not require current input, generate heat, and are cheap. Khalil et al. fixed the permanent magnet on the end effector of the 4-DOF manipulator, and the maximum magnetic field and magnetic field gradient that could be generated were 85 mT and 1.6 T/m, respectively [53]. Xu et al. control the direction, position, and speed of nanospears by using a neodymium-iron-boron magnet. When the distance between the magnet and nanospears is 2–5 cm, the nanospears can be controlled to turn, and when the distance is 1–2 cm, the nanospears can be controlled to move. With the decrease in the distance, the moving speed of nanospears increases [54]. Yousefi et al. proposed a new driving system that simultaneously controls the plane position of two magnetic microrobots according to the characteristic that a permanent magnet can provide a large magnetic field intensity. When the microrobots move far enough, the interaction force between the microrobots can be ignored compared with the force exerted on the microrobots by the rotating permanent magnet. It is proved effectively by simulation and experiment results [55]. Zhan et al. designed a controllable magnetic guide wire made of commercial guide wire, Ecoflex, and magnetic powder. The magnetic control system is mainly composed of programmed control motors and permanent magnets. It has a 700 mm × 500 mm × 500 mm working space and enough flexibility to meet the requirements of surgical operations [56]. As shown in Fig. 2A, Zarrouk et al. built an actuator with a four-piece permanent magnet system and combined it with the

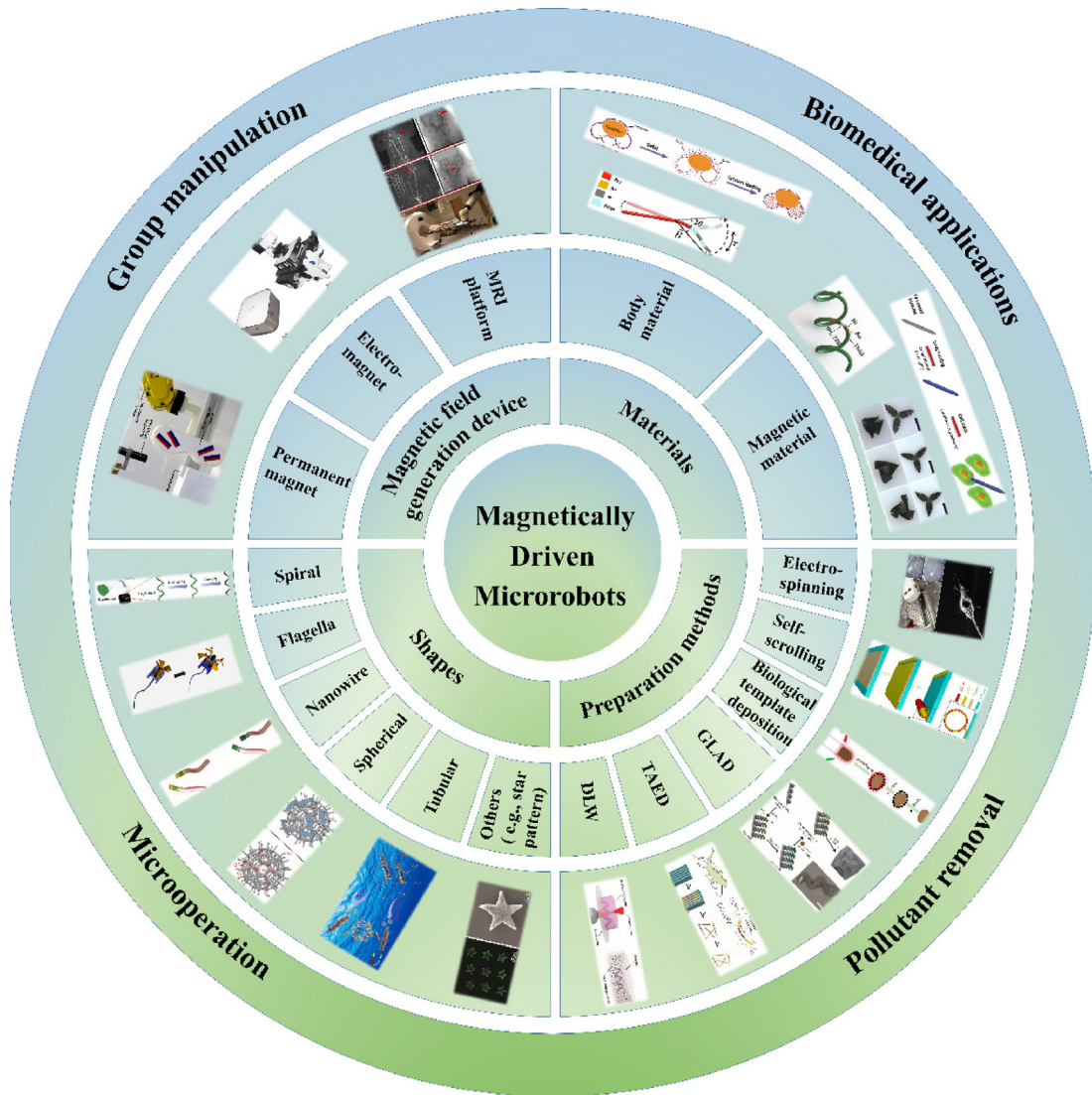


Fig. 1. The content of this review: includes the magnetic field generating device, microrobot materials, shapes, preparation methods, and applications.

Table 1
A comparison of actuation methods.

Actuation methods		Advantages	Disadvantages	Reference
Permanent magnet		High force/torque Cheap Doesn't generate heat Mature technology	Inconvenient operate Large volume The magnetic fields cannot be turned off at any time.	[19,54,58,74]
Electromagnet	Air core type	Easy to control The magnetic field can be turned off at any time. Mature technology	Low force/torque Small workspace Electricity consumption	[61–68,75–77]
	Iron core type	Easy to control High force/torque Magnetic fields can be turned off at any time.	Low force/torque Small workspace Electricity consumption	[52,78,79]

robotic arm to realize drug delivery in the body. It is worth paying attention that the driving platform is equipped with a hybrid vision system, which can accurately control the position of the actuator relative to the working platform, then the steering control of the microrobot is realized. Based on the principle of spatial superposition of magnetic fields, four permanent magnets are divided into two groups, forming system 1 and system 2. In a two-dimensional plane, system 1 is fixed, and the magnetic field direction of system 2 is changed by adjusting its position and direction.

When the angle of the magnetic fields generated by the two systems at a certain point in space is 0, the point has the maximum magnetic field. Using this principle, even if there is a slight disturbance in time, the microrobot can be driven to this point, thus realizing the open-loop control of the microrobot [57].

In summary, the use of permanent magnets can provide a strong magnetic field [19,58], and by combining it with the robotic arm [59], the spatial position of permanent magnets can be changed, many automatically operated magnet systems are designed by

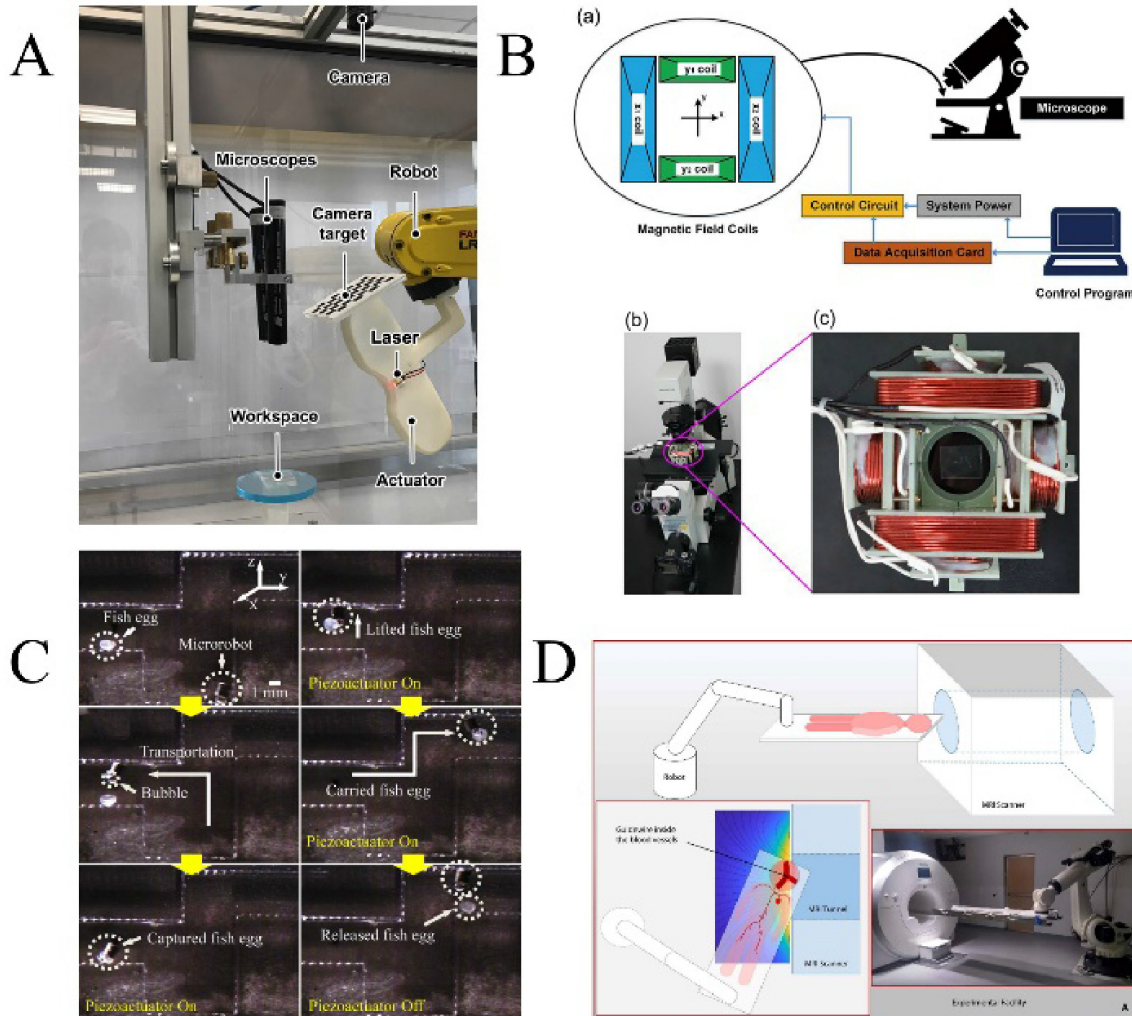


Fig. 2. (A) Permanent magnet actuator and other components of its platform. Reproduced from Reference [57] with permission from Elsevier. B) The composition and components of a magnetic target device. (a) Schematic diagram of the magnetic target device. (b) Stage containing magnetic field coil. (c) Two-axis magnetic field coil. Reproduced from Reference [62] with permission from Elsevier. (C) Capture, transport, and release fish eggs through an electromagnetic drive system. Reproduced from Reference [67] with permission from Elsevier. (D) FNN theory and experimental equipment. Reproduced from Reference [73] with permission from the American Association for the Advancement of Science.

combining magnets with commercial robotic arms, such as Kuka Robotics LBR Med robotic arm [59] and Yaskawa Motor MH5 robotic arm. Permanent magnet drive system uses cylindrical NdFeB permanent magnet fixed on its end effector and robotic arm. Such an integrated system is more reliable and accurate. In addition to the magnetic field gradient, the rotating permanent magnet system consists of magnets, mechanical arms and motors. When the magnets rotate, magnetic torque can also be applied to small-scale equipment [60], which can realize the rotating drive mechanism, thus changing the size and direction of the magnetic field in the working space. However, the commonly needed equipment is rather bulky [55,56], and it is impossible to turn off the magnetic field by turning off the power supply like an electromagnet. In the future, further research is needed in equipment miniaturization and permanent magnet cooperative control.

2.2. Electromagnet actuators

Although permanent magnets have the advantages mentioned above, they need to be accurately positioned and controlled to generate the required magnetic field. Meanwhile, researchers generate magnetic fields through electromagnet. In this way, the required

magnetic field can be generated in real time by applying current. Maxwell coils, which generate a gradient magnetic field, and Helmholtz coils, which generate a uniform magnetic field, are currently used individually or in combination [61]. The current commonly used Helmholtz coil structure is composed of a pair of identical circular conductor coils. The two coils are symmetrically distributed in a Cartesian coordinate system. The coil radius and the distance between the coil center are R , two coils have current in the same direction. The structure of the Maxwell coil is similar to the Helmholtz coil structure. The difference is that the center distance between the two coils is $\sqrt{3}R$, and the two coils have opposite currents. As shown in Fig. 2B, Chen et al. placed a set of electromagnetic coils in the x-direction and y-direction to generate a gradient magnetic field. The current can be controlled by a program to generate focusing, rotating, and oscillating magnetic fields [62]. Sukho Park and his team members used two-axis Helmholtz coils to generate an alternating magnetic field to drive the tadpole-shaped microrobot tail fin to swing and achieve forward motion [63]. Yu et al. use the rotating magnetic field generated by the coil to actuate the Janus microrobot to move on the surface. When a magnetic field with a frequency of 32 Hz and a magnetic field strength of 5 mT is applied, the maximum forward speed

can reach 133 $\mu\text{m}/\text{s}$ [64]. Fu et al. produced a spiral microrobot with a protective cover. When the coil is used to provide 95 mT, the rotation speed of the microrobot is 120 rad/s [65]. They also proposed a magnetic drive system, including a magnetic drive microrobot, a drive system, and a positioning system. The motion of the microrobot is controlled by changing the magnetic field frequency and rotating magnetic field direction, when the frequency is 15 Hz, the maximum moving speed is 2.4 mm/s. The performance evaluation of the system is completed through the motion test of the microrobot [66]. In addition to using the above two types of coils alone, many scientists try to combine the two types of coils [67,68]. The magnetic navigation system made by Jeon et al. consists of two parts. The first part consists of a pair of Helmholtz coils and two uniform saddle coils, which generate a rotating magnetic field. The second part consists of a pair of Maxwell coils and one gradient saddle coil to generate a gradient magnetic field [69]. Chung used the above two coils to design an electromagnetic drive system. The system has a pair of Helmholtz coils and Maxwell coils in the horizontal and vertical directions, through the synergy of magnetic drive and acoustic drive, as shown in Fig. 2C [67]. As shown, fish eggs are captured, transported, and released in the microchannel. Jeong constructs an electromagnetic drive system composed of a pair of Helmholtz coils and a pair of Maxwell coils and combined with an external acoustic drive to jointly complete the delivery and release of drugs [70]. Yuan et al. designed an electromagnetic drive system based on a rectangular coil. Compared with the circular coil, the rectangular coil has a more accurate calculation expression for the calculation of the magnetic field and gradient. The system can be used to control the microrobot with five degrees of freedom [71]. Inspired by the regular tetrahedron, Dai et al. manufactured a drive system with four electromagnets and used the system to generate a triangular waveform gradient magnetic field to realize the spatial drive of the octopus-shaped microrobot [72].

To sum up, electromagnets have been widely used at present because of their convenience in generating and controlling the magnetic field, and the magnetic field can be regulated by the power supply [65,69]. However, the magnetic field intensity generated by traditional air-core electromagnets is generally small, and the working space is also restricted [62,70]. Iron-core electromagnets can generate stronger magnetic fields [72], but the magnetic field analysis of permanent magnets with iron cores still needs further research.

3. Materials and shapes of magnetically driven microrobots

3.1. Materials for the preparation of microrobots

Although different microrobots are composed of different materials, they can be roughly considered to be composed of two parts: the main body material and the magnetic material [22]. [80] With the development of new materials, the research on microrobots has also changed from rigid robots to soft robots to adapt to complex working environments and complete more challenging tasks through their deformation [81].

3.1.1. Body material

Nature provides researchers with a large number of biological inspirations, and a large number of biological and biological hybrid microrobots were created based on algae and bacteria [82]. Algae is widely found in nature and is already used to build microrobots. Different from the general use of dead microalgae, as shown in Fig. 3A, Yasa et al. attached live microalgae *C. Reinhardtii* to magnetic polystyrene (PS) particles and connected them through electrostatic interaction to realize the drive of microrobots [80]. Wang

et al. used the natural spiral structure of *Spirulina (Sp.)* to create (Pd@Au)/Fe₃O₄@Sp-DOX magnetic microrobots [83], as shown in Fig. 3B. Pd@Au is used in photothermal therapy (PTT), and DOX is used for chemotherapy, which enables the synergistic effect of targeted delivery. The surface of Cellulose nanocrystals (CNCs) is rich in hydroxyl groups, which is conducive to the deposition of metal salts and can be widely obtained from nature. Dhar et al. made microrobots through acidification and surface modification of CNCs. The deposited Fe₂O₃ and Pt are used to provide a magnetic drive and bubble drive, respectively [84]. Hair is a kind of natural protein, which has excellent biocompatibility, widely exists in animal skin, and is easy to get. Singh uses human hair as the body material, and coats the surface with superparamagnetic iron oxide nanoparticles to make it magnetic, and uses it to cultivate mesenchymal stem cells. Under the action of an external magnetic field, the mesenchymal stem cells differentiate into bone cells [85]. Pollen is also used to make microrobots because of the hard shell and the larger cavity structure [86,87]. As shown in Fig. 3C (a), Sun et al. encapsulated Fe₃O₄ nanoparticles and drugs in two cavities of pine pollen by vacuum loading to produce a pine pollen-based micromotor (PPBM) (Fig. 3C (b)).

In addition to using natural biomaterials, various artificial polymers have been synthesized for manufacturing microrobot bodies [61,81,88–91]. The photoresist used in lithography technology has been widely used in the manufacture of microrobot bodies. Kim et al. used poly lactic-co-glycolic acid (PLGA) materials to prepare microrobots. PLGA can degrade in vivo, and eventually become water and carbon dioxide. The researchers used a customized electromagnetic drive and near-infrared integrated system to achieve the transportation and release of anti-cancer drugs [91]. Gelatin-methacryloyl (GelMA) hydrogel has cargo biocompatibility because it can be degraded by mold produced by cells, and is currently used for the construction of microrobots. For the treatment of neurodegenerative diseases, Dong et al. built a spiral-shaped microrobot for the transportation of god-level cells and attached magnetoelectric nanoparticles (MENPs) to the outer surface. As shown in Fig. 3D, the microrobot loaded with SH-SY5Y cells is driven by a rotating magnetic field, and the differentiation of SH-SY5Y cells is realized by an alternating magnetic field [81]. Ceylan et al. also used Gelatin methacryloyl (GelMA) to fabricate a spiral microrobot using photolithography technology. The microrobot can be degraded by the matrix metalloproteinase-2 enzyme in the body, and the concentration of MMP-2 in the tumor site in the body will be high [90].

To sum up, when natural biomaterials are selected as the body material [80,84], the structure of the material itself can be used as the basic structure of a microrobot. Moreover, biomaterials have good biocompatibility [93], which is beneficial to the application in the biomedical field. Biomaterials can be degraded in vivo, which can reduce the recycling links of the microrobots.

3.1.2. Magnetic material

Magnetic materials can be divided into diamagnetic (χ less than 0), paramagnetic (χ greater than 0), antiferromagnetic (χ greater than 0), ferromagnetic ($\chi \gg 0$) and ferrimagnetic ($\chi \gg 0$), according to different susceptibility χ . Ferromagnetic and ferrimagnetic materials have been widely used because of their high magnetic susceptibility. If the body material does not have magnetism, the magnetic material needs to be loaded on the body material by physical vapor deposition, dip coating, and other methods. Iron, cobalt [94,95], nickel, and its alloys are commonly used as magnetic materials.

Nickel has been widely used in the manufacture of microrobots due to its strong corrosion resistance, high saturation magnetization, and easy availability [27,96,97]. Kim et al. used the bionic principle to imitate the structure of paramecium and deposited a

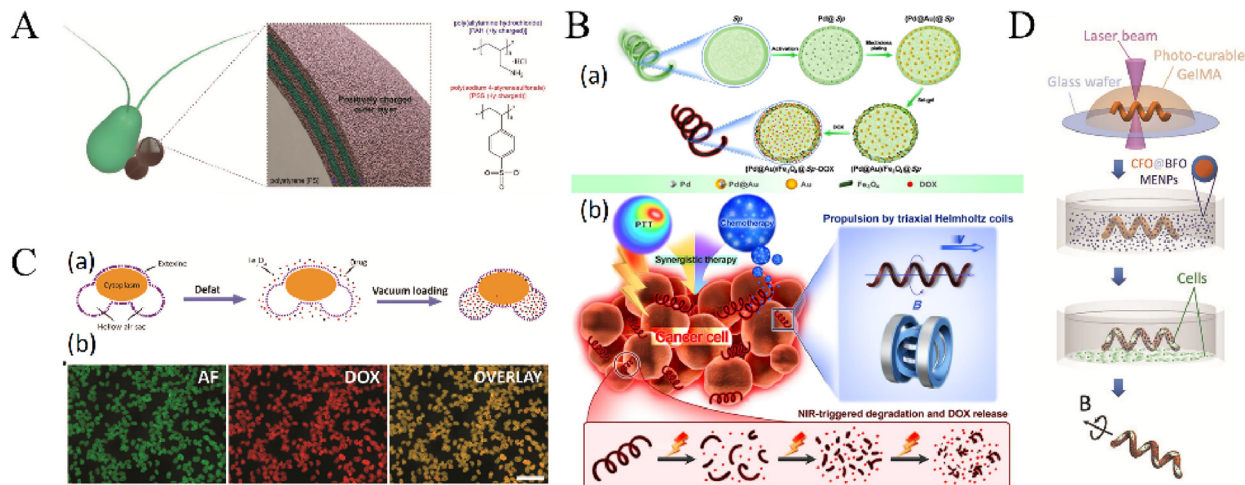


Fig. 3. Typical body materials for constructing microrobots. A) Use electrostatic interaction to realize the combination between microalgae and functionalized particles to make microrobots. Reproduced from Reference [80] with permission from Wiley-Blackwell. B) (a) (Pd@Au)/Fe₃O₄@Sp-DOX manufacturing schematic (b) The microrobot is propelled under the action of a magnetic field, degraded under the action of near-infrared, and released DOX. Reproduced from Reference [83] with permission from the American Chemical Society. C) (a) Schematic diagram of microrobot manufacturing and drug loading. (b) Fluorescence imaging of the drug-loaded DOX microrobot. Reproduced from Reference [92] with permission from the Royal Society of Chemistry. D) Schematic diagram of preparing biodegradable microrobots using TPP. Reproduced from Reference [81] with permission from Wiley-VCH Verlag.

200 nm nickel layer and a 20 nm titanium layer on the cilia to provide magnetic and biocompatibility [98]. As shown in Fig. 4A, Jeon et al. used three-dimensional lithography to fabricate microrobots with four structures: spherical, cylindrical, spiral, and cubic, and sputtered 170 nm nickel and 20 nm titanium layers on the surface for the transportation of stem cells in the body [99]. Using template electrochemical deposition technology, Zhang et al. produced nickel nanowires. The nickel nanowires caused the surrounding

liquid to flow under the action of a rotating magnetic field, thereby realizing the non-contact manipulation of polystyrene beads [100].

However, studies have found that nickel ions are harmful to the human body. Iron and its compounds have been widely used in the manufacture of microrobots [61,104–106]. As shown in Fig. 4B, Srivastava et al. extracted calcified porous microneedles from dracaena and coated the surface with a layer of Fe-Ti for drug delivery in the body [101]. The Nelson team combined laser direct

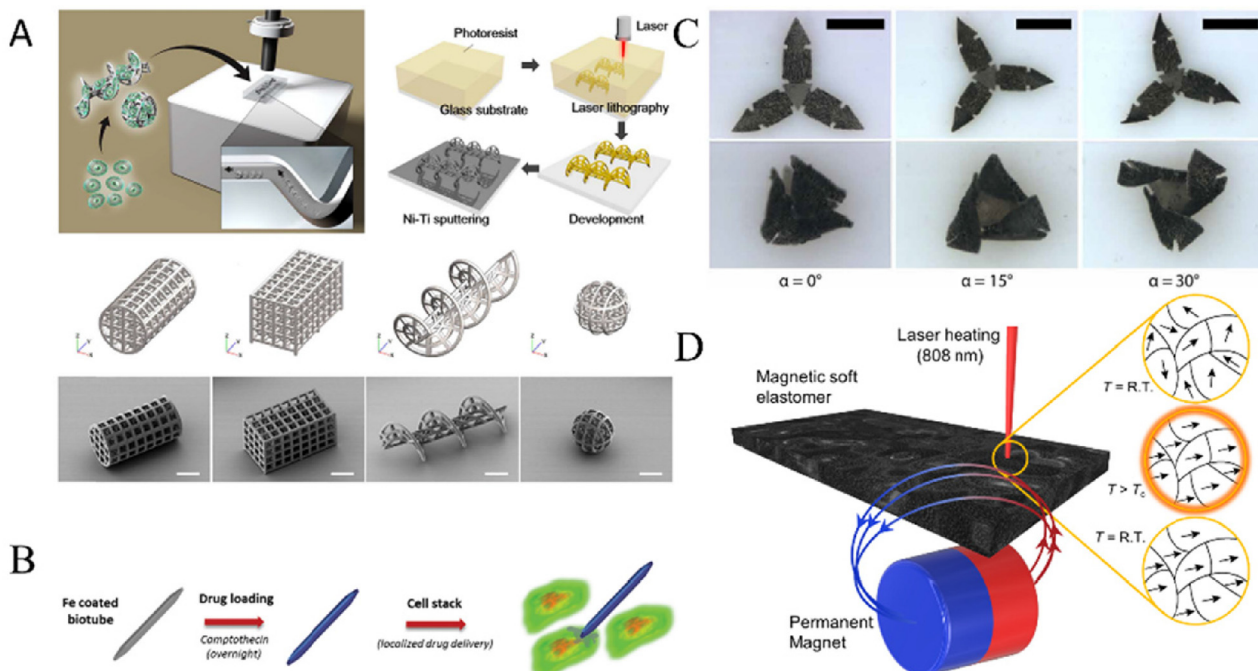


Fig. 4. Typical magnetic materials for constructing microrobots. A) Use photolithography technology to manufacture microrobots of various shapes and plate nickel on the surface. Reproduced from Reference [99] with permission from the American Association for the Advancement of Science. B) The surface of the microrobot is plated with Fe and used for drug delivery. Reproduced from Reference [101] with permission from Wiley-Blackwell. C) Microrobot deforms under the action of a 20 T external magnetic field. Reproduced from Reference [102] with permission from the American Association for the Advancement of Science. D) Schematic diagram of using laser and external magnetic field to change the magnetization direction of Cr₂O₃. Reproduced from Reference [103] with permission from the American Association for the Advancement of Science.

writing technology and template electrodeposition technology to create ferromagnetic microrobots with various shapes, the coercivity of the microrobot was 350e and the saturation magnetization was about 1.2 T [107]. Tang et al. used microfluidic template synthesis, biosilicification, and controlled cutting to create a hollow spiral structure. The rigid Fe_3O_4 structure produced has good mechanical strength and transport efficiency [108]. Pumera et al. used Fe_3O_4 , photoactive (BiVO_4), and other materials to produce $\text{Fe}_3\text{O}_4@\text{PEI/BiVO}_4$ microrobots to remove bacteria generated by dental implants in the mouth under the action of a transverse rotating magnetic field [35]. Xu et al. used ultraviolet lithography to wrap NdFeB permanent magnetic particles in UV resin, and the direction of the magnetic particles in UV resin can be repositioned by changing the external magnetic field. The programming of magnetic particles [102] realizes the deformation of the micro-robot by applying different magnetic field strengths, as shown in Fig. 4C. For the same research on programmable, as shown in Fig. 4D, Alapan et al. embed CrO_2 into PDMS and use thermally assisted magnetization technology to program microrobots, specifically, using lasers to heat materials to a temperature above the Curie temperature. During the cooling process, the direction of the magnetic domains is redirected by an external magnetic field. When a magnetic field of 60 mT perpendicular to the plane is applied, the six-legged microrobot transforms into a complex three-dimensional structure [103].

To sum up, traditional permanent magnet materials (Fe-Co-Ni permanent magnet materials), ferrite permanent magnet materials, and NdFeB have been widely used [102,109]. And magnetic nanomaterials represented by Fe_3O_4 are also widely used because of their low cytotoxicity [35,108]. When selecting magnetic materials, it is necessary to ensure that they have large remanence B_r and maximum magnetic energy product $(BH)_{max}$ and can realize rapid response to the magnetic field [107].

3.2. The shape of the microrobot

As mentioned above, according to different driving methods and application fields, microrobots are designed into different structural forms, including spiral shapes inspired by nature and independently designed spiny spheres. And with in-depth research

on processing methods and driving principles, various shapes of microrobots have also been developed. Table 2 summarizes shapes, fabrication methods, materials, dimensions, and applications of typical magnetically driven microrobots.

3.2.1. Spiral

According to the principle of bionics, researchers have also manufactured artificial microrobots on a large scale through technologies [89,121]. Artificial bacterial flagella (ABFs) have been widely used in in vivo and in vitro studies. The external magnetic field rotates and exerts torque on the spiral structure to realize the rotational movement of the object. When the direction of the magnetic field is opposite, the microrobot will perform reverse propulsion [122]. Driven by a rotating magnetic field, the spiral microrobot has a step-out frequency. Ghosh et al. found that in a small-scale range, the step-out frequency is scaled by L^3 [123]. When the rotation frequency of the added magnetic field reaches the step-out frequency, the microrobot can reach the maximum forward speed. When this frequency is exceeded, the maximum torque provided by the magnetic field cannot overcome the viscous resistance, and the forward speed will decrease. Spirulina has been widely used in the commercial field as a nutrient. It naturally has parameters such as helix angle and helix diameter of the helix structure, making it an ideal spiral template [111,124]. Morozov et al. have carried out a theoretical analysis of spiral propulsion and proposed a parameter γ used to judge maneuverability [125]. Yan et al. used spirulina as a biological template to create porous and hollow spiral microcones. The manufactured spiral microcone is superparamagnetic. Due to the hollow structure, the spiral microcone has an ultrahigh-specific surface area (SSA). The SSA of TSA-2-R1 reaches $55.22\text{m}^2\text{g}^{-1}$. The super high SSA value is conducive to the loading of cargo [124]. On this basis, as shown in Fig. 5A, researchers from the same research group produced a spiral structure by depositing Fe_3O_4 nanoparticles on the surface of Spirulina [111].

In addition to the standard straight spiral structure, a spiral structure with a spiral cone angle has also been developed to increase swimming speed [126]. As shown in Fig. 5B, Wu et al. used femtosecond vortex beams to quickly manufacture a hollow spiral structure with adjustable height, diameter, and cone angle. Com-

Table 2
Shapes, fabrication methods, materials, dimensions, and applications of typical magnetically driven microrobots.

Shapes	Fabrication methods	Materials	Dimensions	Applications	Maximum speed	Reference
Spiral	Rapid precipitation technique	TPU, Fe_3O_4	Length: 640 μm	Drug delivery	35.7 mm/s	[110]
	Biological template deposition method	Spirulina platensis, Fe_3O_4		Imaging-guided therapy	85 $\mu\text{m}/\text{s}$	[111]
	Two-photon polymerization	IPL-780, Ni, Au, Thiol		Targeted drug delivery	63 $\mu\text{m}/\text{s}$	[112]
Flagella	Electrostatic self-assembly	sperm cells, magnetic nanoparticles	Length: ~60 μm	Drug delivery	$6.48 \pm 4.1 \mu\text{m}/\text{s}$	[39]
	3D laser lithography	PEGDA, PETA, Fe_3O_4		Precision medicine, Drug delivery	16.3 $\mu\text{m}/\text{s}$	[113]
Rigid-flexible nanowire	Electrodeposition	PPy, Au, Ni, PAH, PSS	Length: 15.5 μm		0.93 body-lengths/s	[114]
	Electrodeposition	PPy, Au, Ni, PVDF		Drug delivery	3 $\mu\text{m}/\text{s}$	[115]
Spherical	Three-dimensional laser lithography	Su-8, Ni, Ti	D = 70–90 μm	Cell transportation		[88]
	React in situ	Fe_3O_4 , $[\text{Fe}(\text{CN})_6]^{4-}$				
Tubular structure	TAED	PPy, PDA, Ni, <i>E. coli</i>	Length: 9–15 μm	Targeted treatment	$1195 \pm 29 \mu\text{m}/\text{s}$	[116]
	TAED	ZIF-8, MnO_2 , $\gamma\text{-Fe}_2\text{O}_3$, Al_2O_3		Cargo delivery	$5 \pm 1 \mu\text{m}/\text{s}$	[117]
Other shapes	Digital light processing (DLP) printing	PEGDA, Fe_3O_4 MNPs	Length: 110–130 μm	Water Remediation	152 $\mu\text{m}/\text{s}$	[118]
	TAED	Ni, Ag, Au,				
				Interactive and synergistic motion		[119]
				Nanoscale manipulation and assembly	59.6 $\mu\text{m}/\text{s}$	[120]

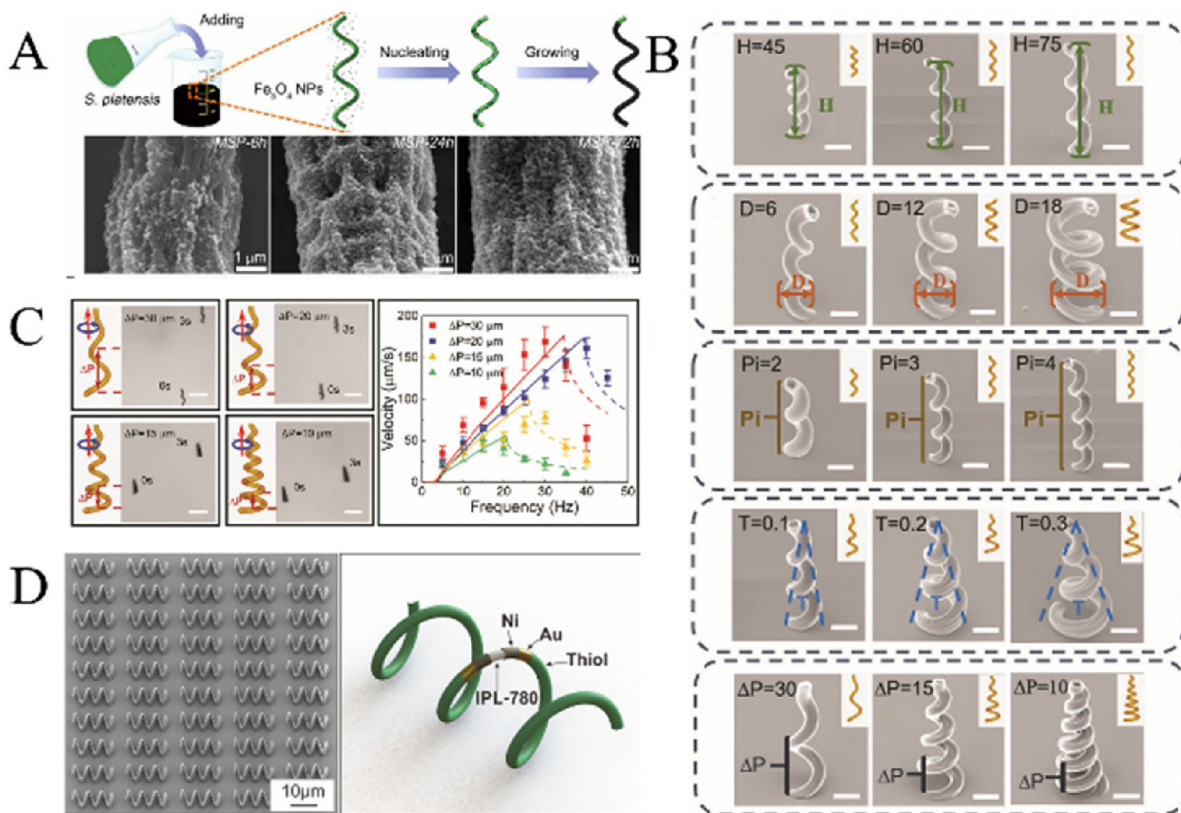


Fig. 5. Manufacturing and modification of spiral microrobots. A) Using algae to prepare spiral-shaped microrobots, the immersion time is 6 h/24 h/72 h respectively. Reproduced from Reference [111] with permission from the American Association for the Advancement of Science. B) Manufacture spiral microrobots with different spiral parameters, including heights H, diameters D, pitch numbers Pi, taper angles T, and pitch periods ΔP . Reproduced from Reference [126] with permission from Wiley-Blackwell. C) The motion status and step-out frequency of spiral microrobots with different ΔP . Reproduced from Reference [126] with permission from Wiley-Blackwell. D) Microrobot coating structure and SEM image. Reproduced from Reference [112] with permission from the American Chemical Society.

pared with the straight micro-helices, the conical spiral forward speed has been increased by 50 %, and the lateral drift has been reduced by 70 %. It is found that those with a longer pitch period have a higher forward speed, the best pitch is 20–30 μm , and the maximum forward speed can reach 180 $\mu\text{m/s}$, the motion status and step-out frequency of spiral microrobots with different ΔP are shown in Fig. 5C. The inner and outer surfaces of the spiral microcone can be loaded with various cargo at the same time, which improves the carrying capacity [126]. Chen et al. combined the manufactured magnetron microcones with piezoelectric material poly-L-lactic acid (PLLA) to create a spiral structure, which was used to carry PC12 cells. After arriving at the designated location, differentiation was induced by ultrasound, and after 7 days, axons were visible [127]. As shown in Fig. 5D, Wang et al. used two-photon lithography to create a spiral microrobot. The microswimmers were functionalized with thiol- and thioether-based compounds and chemical modification was used to improve the hydrophobicity of the surface. It is found that as the hydrophobicity of the surface increases, the water contact angles on the surface of the microrobot become larger, and a higher step-out frequency and faster forward speed are obtained. Surface chemical modification of microrobots has become an important method to improve the propulsion speed [112]. To improve the motion speed of the microrobot in viscous liquid and explore the motion condition of the microrobot in blood, Wie et al. selected a helical microrobot made of thermoplastic polymer nanocomposite material with a swimming speed of 35.7 mm s^{-1} [110]. Sun et al. used shape memory polymers (SMPs) to prepare spiral-shaped microrobots that can be transformed from temporary to permanent shapes under ther-

mal stimulation. This 4D structure has greater potential for work in different environments [128].

To sum up, spiral microrobot has been widely used. In the future, it is necessary to further improve the step-out frequency and movement speed of the microrobot [111,126] by modifying the preparation materials and the surface of the microrobot. It is also an important direction to improve the structure of the spiral microrobots and increase the loading capacity in the future [112].

3.2.2. Flagella

Flagella-like microrobots are another classic structure that humans have drawn inspiration from the natural world [129]. The sperm of mammals achieve undulating propulsion by flapping the flexible flagella of their tails [82,130,131]. Magdanz et al. have studied the kinetics of sperm movement in the tube, and for the first time established a connection between the parameters of the tube and the motility characteristics of the sperm, and provided theoretical guidance for the study of sperm motility [132]. As shown in Fig. 6A, Magdanz and his team members fabricated the IRONSperm microrobot using an electrostatic-based self-assembly method. The speed of movement is proportional to the frequency of the magnetic field. When the driving frequency and the precession angle are 8 Hz and 45°, the movement speed can reach 0.2 length/s [39]. Different from the use of dead sperm, Xu et al. used live bovine sperm to create a microrobot for drug delivery. The microrobot is composed of bovine sperm and a magnetic microstructure. Bovine sperm provides driving power, and the magnetic microstructure is carried out under the action of an external magnetic field [129]. As shown in Fig. 6B, Xu et al. used

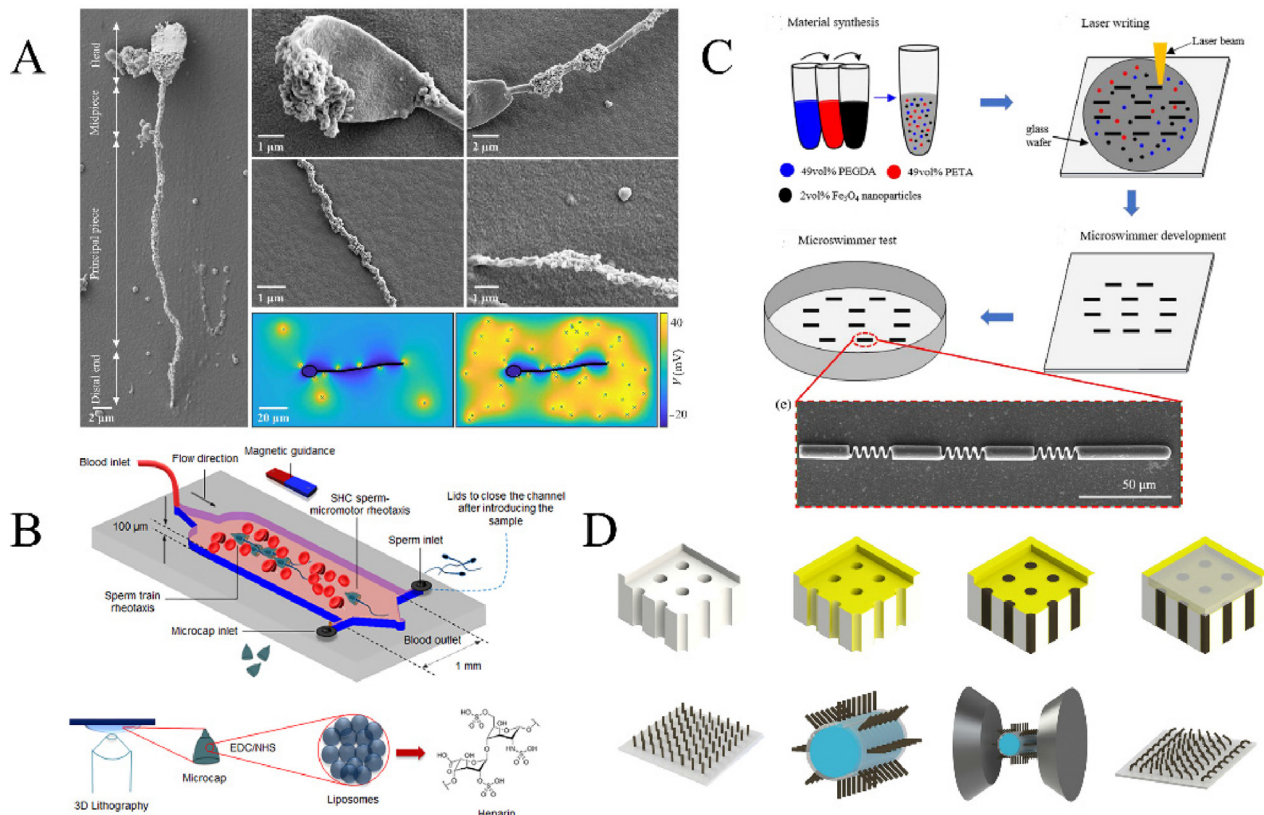


Fig. 6. Manufacturing of typical flagellar microrobots. A) The attachment of magnetite nanoparticles to sperm. Reproduced from Reference [39] with permission from the American Association for the Advancement of Science. B) Conceptual schematic diagram of using magnetic force to drive SHC sperm micromotor to move in the blood. Reproduced from Reference [40] with permission from the American Chemical Society. C) Manufacturing process of a new type of microrobot with a four-stage rigid structure. Reproduced from Reference [113] with permission from MDPI (Basel, Switzerland). D) Schematic diagram of manufacturing and magnetization of artificial cilia-shaped microrobots. Reproduced from Reference [109] with permission from Springer Nature.

sperm to manufacture streamlined-horned cap (SHC) hybrid sperm micromotors, which realized the simulation of the movement against the direction of blood flow in the microfluidic chip. Depositing iron on the microrobot SHC at an angle of 75° and applying a uniform magnetic field can realize the self-assembly of the microrobots to form a chain structure, which can realize the group control of the microrobots [40]. To improve biocompatibility and equipment integrity, as shown in Fig. 6C, based on the principle of undulatory propulsion, Zhang and his team prepared a solution using poly(ethyleneglyco) diacrylatd (PEG-DA), pentaerythritol triacrylate (PE-TA) and Fe_3O_4 nanoparticles. And a new type of microswimmers is manufactured by two-photon lithography technology. The structure consists of four rigid sections connected by springs. Under the excitation of the oscillation frequency, the heads of the microswimmers are regularly bent up and down, which in turn drives the other parts to fluctuate [113]. In recent years, with the study of creatures with a large number of hairs in nature, it has been found that they drive their motion through metachronal waves. Compared with the synchronized motion of cilia, this mode of motion has a higher propulsion efficiency. As shown in Fig. 6D, Gu et al. manufactured magnetic cilia carpets. By changing the direction of the rotating magnetic field, the cilia can be programmed. In the test on the rigid plastic surface, it is found that the carpet will have different movement modes under different magnetic field strengths. When the magnetic field is greater than 60mT, the carpet can be rolled up and achieved rolling motion under the action of the magnetic moment. The in-depth study of this structure will help to develop more promising micro-robots in future research [109].

To sum up, under the action of the magnetic field, the flagella microrobot mainly pushes forward by swinging itself [129]. However, due to the limitation of swing frequency and amplitude, the movement speed of the flagella microrobot has always been a research focus [109]. In the future, we should improve the flagella structure and materials of microrobots and improve their motion characteristics [131].

3.2.3. Rigid-flexible nanowire

Based on the research on the structure of flagella, researchers have fabricated various nanowire structures [114,115]. Nelson et al. fabricated a microrobot with a composite multichain nanowire structure. The nickel section at the head of the structure and the polypyrrole (PPy) section at the tail are connected by a flexible polymer hinge. The manufactured 3-link structure shows a motion form similar to S-like, with a maximum movement speed of 0.93 body-lengths/s [114]. On this basis, other members of the team fabricated hybrid Ni-Ppy-P (VDF-TrFE) nano-eels. The head material is PPy material and a nickel layer is used. The cover provides magnetic properties, and the flexible tail is made of polyvinylidene fluoride (PVDF) copolymer, as shown in Fig. 7A(a). By changing the magnetic field strength and the rotation frequency, nano-eels show three different motion modes, respectively, roll, swing, and spiral motion. Nano-eels are pre-treated with PDA, and rhodamine-B (RhB) is used to simulate drug loading. Nano-eels can be driven by applying a magnetic field and a frequency of 10 mT and 11 Hz. When applied the magnetic field and frequency are 10 mT and 7 Hz, the release of RhB is achieved, as shown in Fig. 7A(b). The release of DOX is verified in vitro [115].

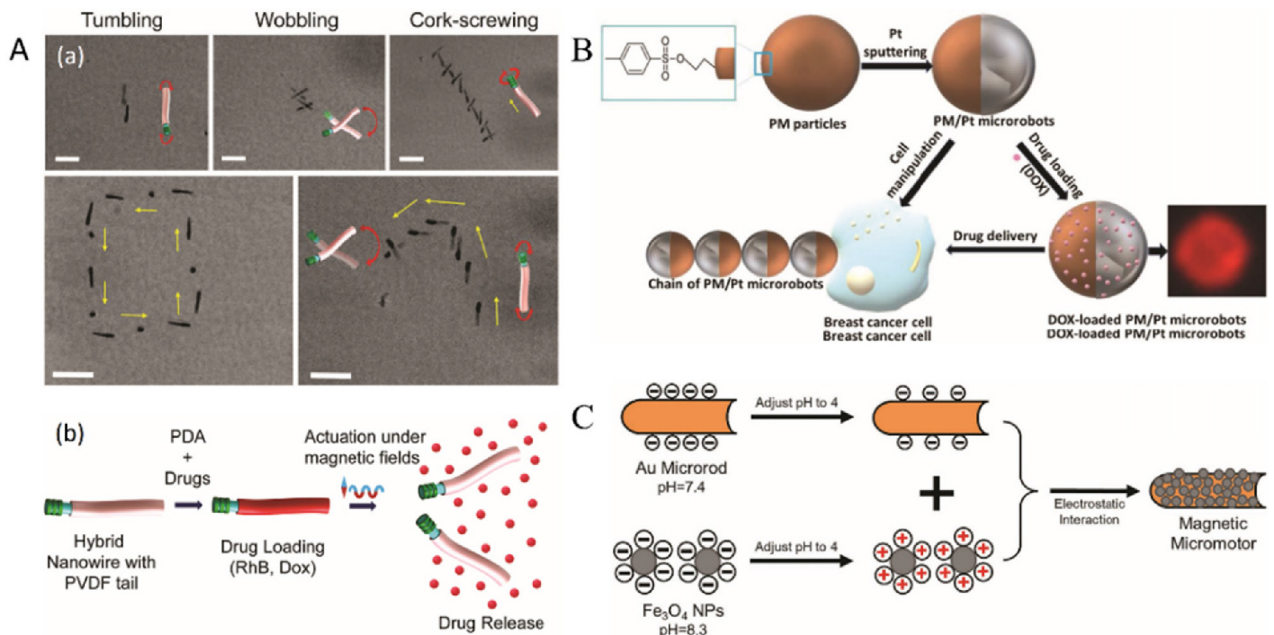


Fig. 7. A) (a) Three motions (tumbling, wobbling, cork-screwing) of the microrobot under different magnetic field strengths and rotation frequencies. (b) Using a magnetic field to control the movement of a flexible microrobot. Reproduced from Reference [115] with permission from Wiley-VCH Verlag. B) Schematic diagram of microrobots for cell manipulation and drug delivery. Reproduced from Reference [135] with permission from Wiley-VCH Verlag. C) Schematic diagram of one-step preparation of tubular micromotors. Reproduced from Reference [28] with permission from Wiley-VCH Verlag.

The nanowire structure developed based on flagella shape can make more forms of motion, which will help to expand its application range. In the biomedical field, the nanowire structure is also beneficial to enter blood vessels and other parts, and the nanowire can be turned by magnetic field control, which is convenient for examination and treatment. In the future, it is still necessary to study the structure and materials of nanowires to realize the more complex movement of nanowires.

3.2.4. Spherical

Li et al. studied the surface motion of Janus microspheres driven by an oscillating magnetic field. Under the magnetic dipole-dipole interaction, two microspheres attract each other to form a dimer. Under the action of an oscillating magnetic field, the dimer can realize the asymmetric rolling of two microspheres on the solid surface, produce a net displacement, and realize forward movement [133]. Joseph Wang promoted Janus microspheres with asymmetric density through acoustic-magnetic synergy. As the coating thickness increases, the speed of the microrobot also increases. Among the various coating thicknesses, the microrobot with a coating thickness of 30 nm Ti has the slowest movement speed, with a speed of 5 $\mu\text{m}/\text{s}$ [27]. Jurado-Sánchez also studied the advancing speed of Janus microspheres. They deposited different materials on polystyrene (PS) microspheres sputtered with a gold layer to make microspheres, and added Pt or MnO₂ nanoparticles, Fe₂O₃ nanoparticles, and quantum dots (QDs). Janus microspheres have bubble drive, magnetic drive, and light drive capabilities. Compared with bubble-magnetic mode, the propulsion speed of the bubble-magnetic mode can be increased by 3 times [134]. The Janus microspheres manufactured by Vila et al. are composed of iron oxide particles inside and an outer tosyl group. As shown in Fig. 7B, the loading of DOX is realized by covalent bonding, and the microrobot can be assembled by using a weak magnetic field. It is a chain structure, and then manipulates breast cancer cells (T47D cell line) [135].

To sum up, the spherical structure is convenient for manufacturing. The two hemispheres of Janus spheres usually have different surface properties, and the movement of microrobots

can be realized through asymmetric movement. By combining with other driving methods, higher driving efficiency can be achieved. The modification of the spherical surface is still an important research direction in the future, and the combination with other driving methods can broaden the working range of the spherical microrobot. Zheng et al. used Fe₃O₄ and [Fe(CN)₆]⁴⁻ to prepare spherical ROS-scavenging nano-robots (ROSrobots) in an acidic environment, and the Prussian blue produced on the surface can clear reactive oxygen species (ROS) in vivo [116].

3.2.5. Tubular structure

The tubular structure has the advantages of a simple structure [118,136], is easy to manufacture, and is convenient to equip cargo. Li et al. adjusted the pH to 4 to make the paramagnetic Fe₃O₄ nanoparticles and gold micro rods carry positive and negative charges, respectively. The Fe₃O₄ nanoparticles were attached to the surface of the gold micro rods through electrostatic attraction, as shown in Fig. 7C. The rod-shaped microrobot is manufactured in one step, and Fe₃O₄ nanoparticles are extremely acid resistant. Even if they are immersed in a solution with a pH of 0.9 for 24 h, the microrobot still has cargo magnetic manipulation capabilities [28]. The Sánchez team successfully captured a single *E. coli* bacteria with PDA-modified microtubules and created a biohybrid microrobot. This is the first proof of concept of the bacteria-microtubule model. When the task is completed, to inhibit the activity of *E. coli* and prevent the reproduction of *E. coli*, the researchers created a “kill switch” by covalently binding urease on the surface of the PDA. When the microrobot completes its task, it can decompose urea to produce NH₃ through an enzymatic reaction, and then change the local pH value to achieve the inhibitory effect of *E. coli* activity [117]. And the tubular structure is convenient to manufacture and can be obtained in large quantities. By modifying the inner and outer surfaces, different goods can be loaded separately, which is beneficial to improve transportation efficiency. In the future, research on the tubular microrobot will mainly focus on the surface structure and application, and the multifunction of the tubular structure will be realized by improving the surface structure.

3.2.6. Other shapes

With the study of the driving mechanism of microrobots by researchers, various new and unique geometric structures have been developed. Li et al. created multilinked two-arm nano swimmers, as shown in Fig. 8A, the microrobot is driven by an oscillating magnetic field through a driving method similar to human freestyle. Under the oscillation frequency of 25 Hz, the maximum advancing speed can reach 59.6 $\mu\text{m}/\text{s}$ [120]. Liao et al. used 3D printing to manufacture rigidly segmented microrobots, as shown in Fig. 8B, a nickel layer is deposited on the head of the microrobot, and the head oscillates under the action of a magnetic field, which in turn drives the rigid structure behind to swing to achieve wave propulsion [137]. As shown in Fig. 8C, Hu et al. injected a mixture containing poly(vinylalcohol) (PVA), alginate (ALG), magnetic nanoparticles, and DOX into a silicon plate with a star pattern, and by introducing calcium ions to make it gel. A horizontal rotating magnetic field is used to realize the rotation of the microrobot. By applying a rotating magnetic field in the vertical direction, the friction force generated by the microrobot and the glass slide is to drive forward movement, reaching a maximum speed of 17 $\mu\text{m}/\text{s}$ at the step-out frequency [138]. Specific movement can be realized by its unique structure. It is an important research direction in the future to make a new type of microrobot with a bionic principle. Zhu et al. prepared a gear-shaped microrobot, which rotated under the action of a rotating magnetic field. The magnetic field frequency corresponding to the maximum rotational speed is the critical frequency (c_f). By applying rotating magnetic fields of different frequencies, the interaction and cooperative behavior between multiple robots can be realized [119].

4. Manufacturing method of the magnetically driven microrobot

The rapid development of microrobots benefits from the rapid development of micro-electromechanical systems (MEMS) technology. At present, it has great research potential in the fields of

biomedicine, environmental monitoring, and nano-micro-mixed technology [139]. MEMS processing technologies include lithography, ion implantation, diffusion, oxidation, sputtering, corrosion, and LIGA. A combination of one or more technologies can be used to fabricate a microrobot. Table 3 summarizes manufacturing methods and their advantages and disadvantages.

4.1. Biological template deposition method

The biological deposition method is a commonly used method for the manufacture of biohybrid microrobots [140–142]. The body structure is manufactured by physical and chemical treatment of materials from nature, and magnetic materials are added to the body structure to manufacture the microrobot by dipping, physical vapor deposition, and other methods. The use of various spores of nature, spirulina, etc. as biological templates to manufacture microrobots has been extensively studied, which provides a reliable method for solving biocompatibility. As shown in Fig. 9A, Zhang et al. produced a new type of biological hybrid adsorbent. After hydrothermal treatment, Fe_3O_4 nanoparticles were deposited on the surface of Ganoderma lucidum spores to produce organic/inorganic porous spore@ Fe_3O_4 biohybrid absorbents (PSFBAs). With the deposition of nanoparticles, the surface of PSFBAs has a larger specific surface area and more negative charges, which is conducive to improving its adsorption capacity [140]. As shown in Fig. 9B, Zhang et al. fabricated a fluorescent magnetic spore-based (spore@ Fe_3O_4) by depositing Fe_3O_4 nanoparticles on the surface of Ganoderma lucidum spores and binding functionalized fluorescent carbon dots (CDs) to the surface of the spores as sensing probes. Manufactured fluorescent magnetic spore-based (spore@ Fe_3O_4 @CDs) microrobots (FMSMs). Due to the introduction of Fe_3O_4 and CDs, the Brunauer-Emmett-Teller surface area of FMSMs is $12.96 \text{ m}^2/\text{g}$. The introduction of CDs can provide fluorescence imaging for in vivo tracking, and the manufactured FMSMs can be used to detect *C. diff* in culture liquid and even stool samples [141]. Using the spiral-shaped xylem catheters of vascular plants,

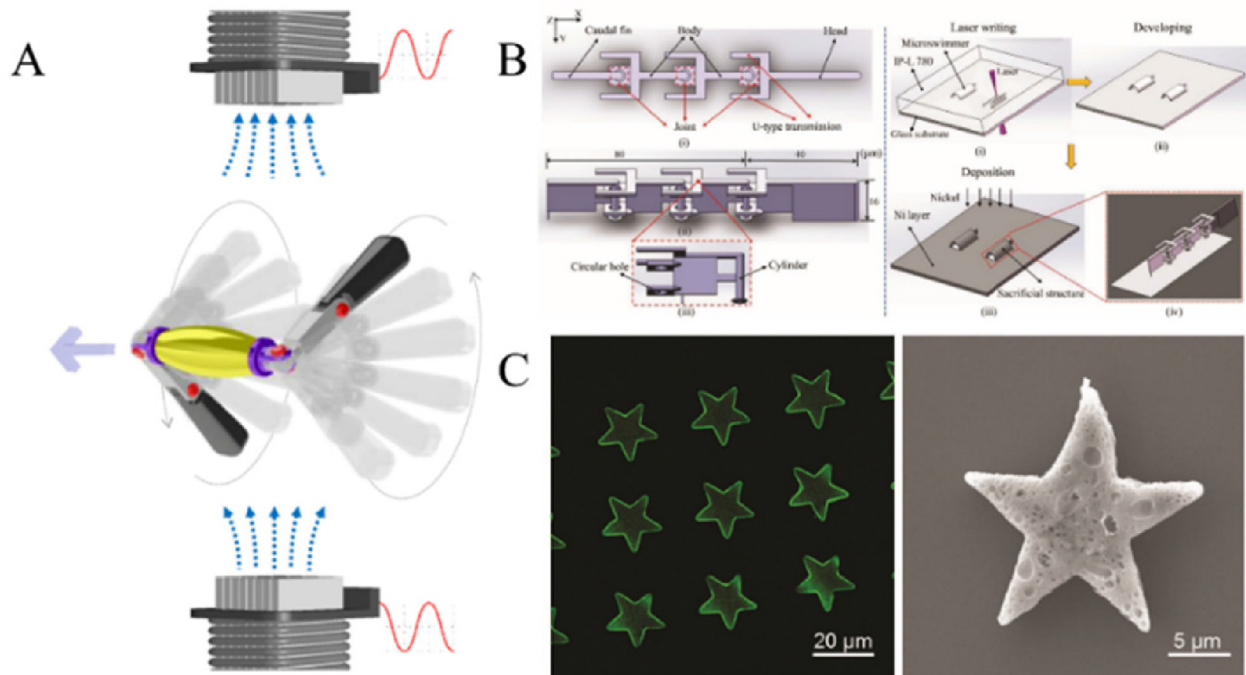


Fig. 8. A) A microrobot similar to human freestyle swimming moves under the action of an oscillating magnetic field. Reproduced from Reference [120] with permission from the American Chemical Society. B) Design prototype and manufacturing steps of the rigid-shaped microrobot. Reproduced from Reference [137] with permission from Wiley-VCH Verlag. C) SEM and EDX images of the star-shaped microrobot. Reproduced from Reference [138] with permission from Wiley-VCH Verlag.

Table 3
A comparison of manufacturing methods.

Manufacturing method	Advantages	Disadvantages	Reference
Biological template deposition	Easy to operate High yield Rapid to manufacture	Limited shape control Special materials	[140–142]
Direct laser writing	Good size control High yield Rapid to manufacture	Requiring professional equipment Higher requirements for operation	[89,96,122,143,144,146,166]
Template-assisted electrochemical deposition (TAED)	Easy to operate Rapid to manufacture Good size control	Special materials Higher requirements for operation	[148–151,157]
Glancing angle deposition (GLAD)	High yield Good size control	Requiring professional equipment Higher requirements for operation	[154–156]
Self-scrolling technique	Easy to operate	Limited shape control Higher requirements for operation	[159–161,167]
Electrospinning technology	Low cost Rapid manufacturing	Higher requirements for operation Slow speed	[21,162–165]

as shown in Fig. 9C, Gao et al. created a biohybrid microrobot [142]. The diameter and pitch of the spiral structure can be controlled by mechanical stretching, which is conducive to the mass production of microrobots with different spiral parameters, during cutting, the nickel and titanium layers deposited on the surface are beneficial to protect the spiral structure. Although the method of biological template deposition has been widely used, how to achieve uniform coverage of surface magnetic materials is still one of the key problems that need to be solved at present.

4.2. Direct laser writing

Direct laser writing (DLW) is to irradiate a photopolymer with a pulsed laser and then process the polymer with a developer to obtain the designed structure [143]. As shown in Fig. 10A, Tottori et al. achieved rapid mass manufacturing of spiral microrobots by using 3D laser direct writing and fabricated a microrobot with a microholder head structure for space capture, transportation and release operations of colloidal particles [89]. The two-photon direct laser writing (TDLW) technique also treats liquid materials by laser irradiation, but it needs to be the focus to achieve the curing strength. Compared with traditional photolithography technology, it has a faster processing speed and higher sensitivity. Nelson et al. used this technology to manufacture the microrobot. As shown in Fig. 10B(a), the selected body material is non-toxic photocrosslinkable hydrogel gelatin methacryloyl (GelMA), and place the manufactured microrobot in DI water containing Fe_3O_4 to make it magnetic [144]. One advantage of lithography is that various shapes can be prepared. As shown in Fig. 10B(b), manufactured microrobots of different sizes and thicknesses. Giltinan et al. chose an IP-S photoresist and used two-photon lithography technology to manufacture transchiral micromotors of different specifications and sizes. Using the manufactured spiral B_L and C_R and tapered rod to manufacture configuration I, use A_L and B_R and tapered rod to manufacture configuration II. When a 4 Hz rotating magnetic field is applied, configuration I remains almost stationary, and configuration II advances. When a 7 Hz rotating magnetic field is applied, configuration I advances and configuration II advances in reverse. This realizes that two microrobots can be driven independently in the same space [122]. As shown in Fig. 10C(a), Cabanach et al. prepared zwitterionic photoresists based on two types of zwitterions, carboxy betaine, and sulfobetaine. The microrobot made by two-photon lithography technology was not found by phagocytes in the inspection for more than 90 min (Fig. 10C(b)) and this provides material guidance for the manufacture of microrobots [145]. To combine the excellent properties of metal and polymer materials, the Nelson team recently

combined 3D lithography, mold casting, and electrodeposition technologies to achieve the interlocking of different types of materials. Researchers combine metal structures with polymer frameworks, and different control effects can be achieved by choosing hydrophobic or hydrophilic frameworks [146].

4.3. Template-assisted electrochemical deposition (TAED)

Template-assisted electrochemical deposition (TAED) is also a very widely used method for manufacturing microrobots. It has been widely used in the manufacture of tubular-like [147] and chain-like microrobots. Li et al. used this method to manufacture spiral microrobots with different specifications and sizes. They found that the length and pitch of the microrobots can be controlled by adjusting the charge density and the composition of the plating solution during the manufacturing process. When the composition of the plating solution is 30 mM PbCl_2 , 20 mM CuCl_2 , and 0.1 M HCl, the helical structure has the best performance [148]. The study found that the bending movement of the body and the tail fin of the fish in the water is transformed into a forward movement. As shown in Fig. 11A, Li et al. produced fish-like nano swimmers by imitating the BCF movement. The structure consists of a gold segment on the head, a nickel segment on the body, and a gold segment on the tail connected by a flexible silver hinge. The head of the traditional flagella-shaped microrobot is the active part, and the head swings to drive the body to move, while the fish-like nano swimmer's body is the active part, which drives the head to move through the wave. During the driving process, the body swings can produce the maximum angular velocity. It produces greater bending force for pushing forward, and the maximum forward speed can reach 30.9 $\mu\text{m/s}$ under the driving of the 11 Hz oscillating magnetic field [149]. Mushtaq et al. used this method to manufacture TiO_2 -PtPd-Ni nanotubes (NTs). As shown in Fig. 11B, NTs can be propelled by photo-induced decomposition of H_2O_2 , or they can be driven by applying an external magnetic field, or under the action of a sound field can realize linear motion, which provides a solution for multi-physics collaborative driving [150]. Joseph Wang created a spiral microrobot by combining template electrochemical deposition and electron beam evaporation technology. To make the microrobot evade the recognition of the immune system in the body and increase the running time in the body, the platelet membrane is wrapped outside the spiral structure (Fig. 11D), and the characteristics of the wrapped platelets can be used to achieve the binding of pathogens, such as MRSA252 bacteria [151]. Members of Nelson's team used TAED technology to prepare microrobots. For the first time, they studied the motion of nonhelical multifunctional nanorobots under a rotating magnetic

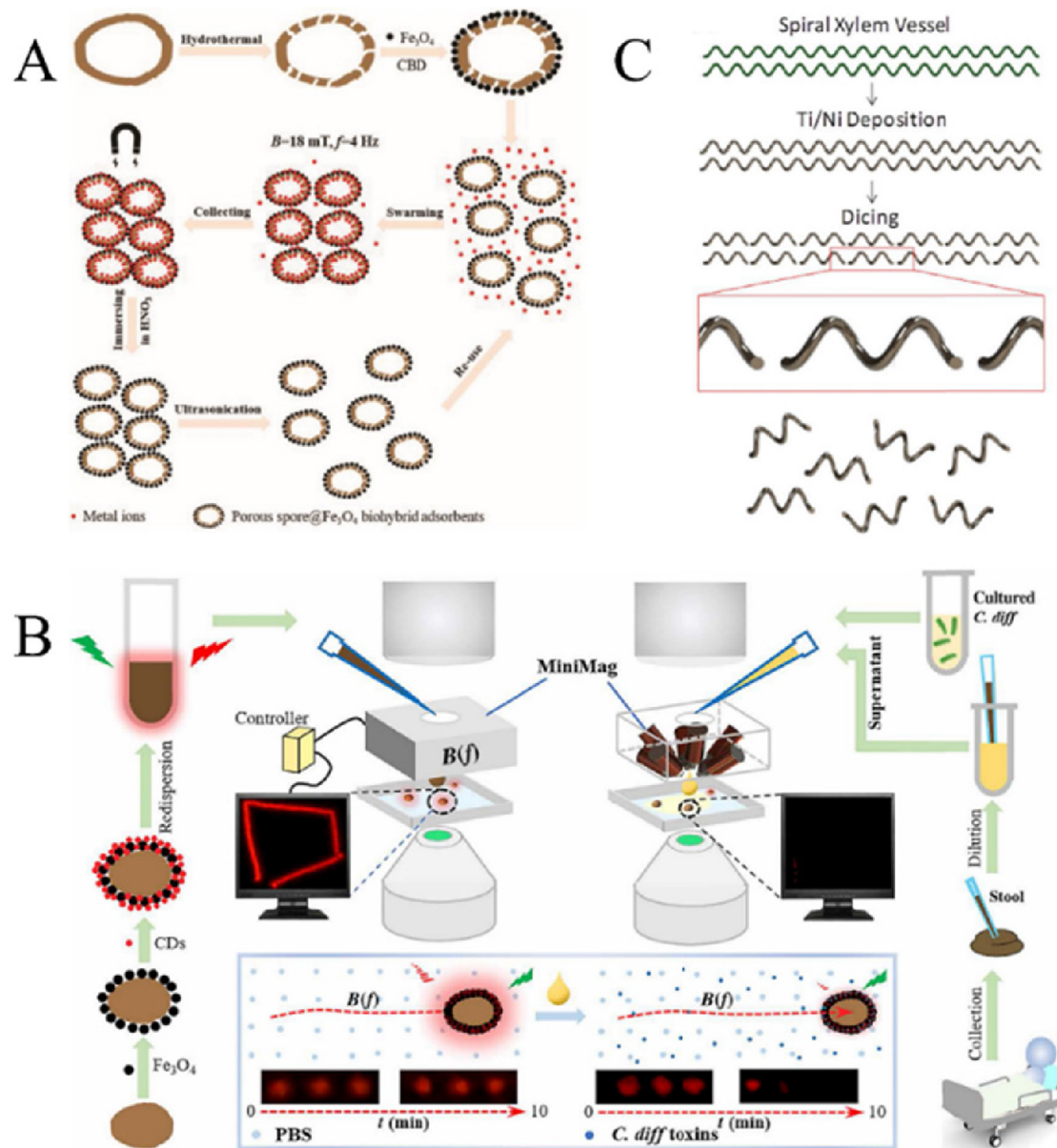


Fig. 9. Preparation of microrobots by biological template deposition method A) Manufacturing of microrobots and removal of heavy metal ions. Reproduced from Reference [140] with permission from Wiley-VCH Verlag. B) The manufacture of FMSMs and the detection of *C. diff*. Reproduced from Reference [141] with permission from the American Association for the Advancement of Science. C) Schematic diagram of manufacturing steps of xylem catheter microrobot based on vascular plants. Reproduced from Reference [142] with permission from the American Chemical Society.

field. By changing the frequency and intensity of the rotating magnetic field, they can realize the rolling motion and spiral bending motion of the microrobots [152].

4.4. Glancing angle deposition (GLAD)

Ophthalmic treatment often requires drugs to work in the eyeball, and the efficacy of drugs through diffusion is difficult to guarantee. Wu et al. used GLAD technology to create spiral microrobots and a microrobot penetrates the vitreous body to reach the retina for ophthalmic treatment [153]. As shown in Fig. 12A(a), Walker et al. also used this method to fabricate a spiral microrobot and plated an 8 nm Al₂O₃ film on the surface of the microrobot by atomic layer deposition (ALD). Microrobots can move in an acidic environment and can penetrate the mucin gel. The researchers attribute this to the fact that urea in the environment is converted to ammonia by urease, which changes the local pH. As shown in Fig. 12A(b), the local

viscosity is reduced due to the gel-sol transition [154]. Schamel et al. used the method of GLAD to create a spiral structure with a diameter of 70 nm. The microrobot can achieve active propulsion in hyaluronic acid. Research suggests that the larger particles of the microrobot in the viscous Newtonian liquid can achieve greater propulsion speed. In the viscoelastic liquid of Hyaluronan (HA), the resistance f is related to the activation barrier, and the small size is conducive to the advancement of speed [155]. Venugopalan et al. used this method to create a spiral microrobot and coated a 150 nm thick zinc ferrite film on the surface with microwave technology, which improved the stability of the magnetic microrobot against agglomeration by an order of magnitude [156].

4.5. Self-scrolling technique

The self-scrolling technique uses coatings of different materials to be deposited on the substrate and employs the internal forces of

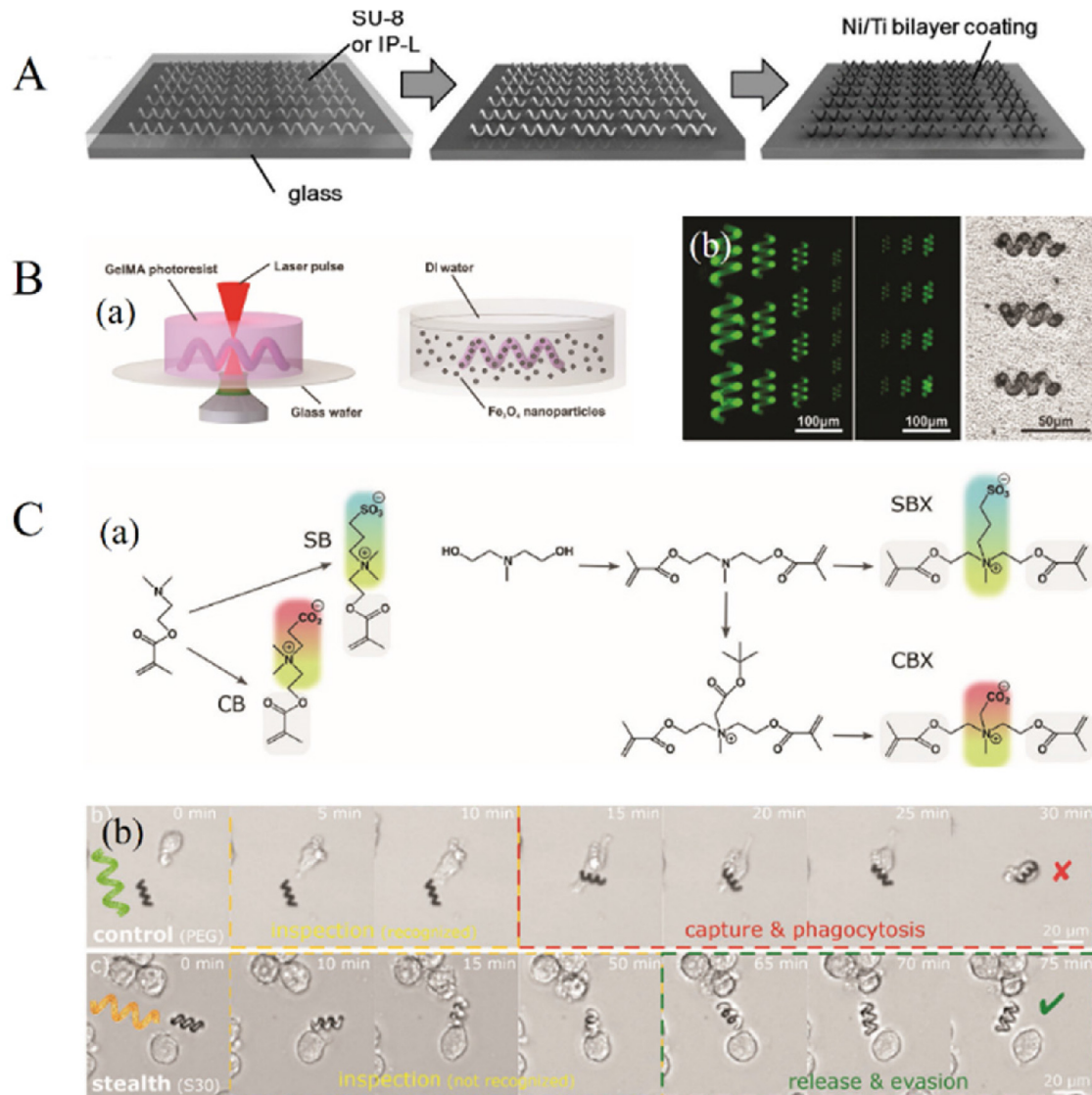


Fig. 10. Lithography technology to manufacture microrobots A) Manufacturing steps of microrobots. Reproduced from Reference [89] with permission from Wiley-Blackwell. B) (a) Schematic diagram of using 2PP to prepare spiral microrobots and attach magnetic particles in DI water. (b) Fluorescence imaging of microrobots of different sizes and different wall thicknesses, and optical imaging of microrobots. Reproduced from Reference [144] with permission from Wiley-VCH Verlag. C) (a) Synthesis of SB and CB monomers, and synthesis of SBX and CBX crosslinking agents. (b) Non-immunogenic invisible microrobot avoids recognition and capture by the immune system. Reproduced from Reference [145] with permission from Wiley-Blackwell.

each layer to achieve self-curling of the coatings to create microstructures [158]. As shown in Fig. 12B, Bradley J. Nelson's team members used self-rolling technology to manufacture ABF [159]. Using the manufactured ABF, the team members manufactured two ABF head sizes, the larger size being 4.5 μm × 4.5 μm × 200 μm, and the smaller one being 2.5 μm × 2.5 μm × 200 μm. The study found that the smaller head has a higher propulsion speed. It is attributed to the smaller size that reduces the viscous resistance, but a larger head can make ABF have a higher step-out frequency and a higher pushing speed [160]. Magdanz et al. prepared microtubule structures with different diameters, lengths, wall thicknesses, and other parameters, and combined them with sperm to produce biological hybrid microrobots [82]. Xi et al. used this technology to manufacture tubular microrobots made of Fe, Cr, and Ti. By controlling the frequency of the rotating magnetic field and the concentration of the solution, the microrobot could be controlled to rotate perpendicular to the pig liver tissue to realize the drilling operation [161].

4.6. Other manufacturing methods

Electrospinning technology has the advantages of low cost, rapid manufacturing, and a simple manufacturing process. It is also used in the manufacture of microtubes and other structures [162–164]. Khalil et al. used electrospinning technology to produce sperm-shaped microrobots ranging in length from 50 μm to 500 μm. When an oscillating magnetic field with a frequency of 10 Hz is applied, the maximum velocity of motion is about one body length per second [165]. Chen et al. combined melt electrospinning writing (MEW), micro-molding, and skiving processes to produce tadpole-shaped microrobots. Rolling and advancing modes can be implemented [164]. Wang et al. made a walnut-like micromotor, which can realize self-propulsion by decomposing H₂O₂ to generate bubbles. Using the hydrophobicity of poly-caprolactone (PCL), when the microrobot contacts the oil, it can collect the oil. Afterward, magnetic force can be used to complete the collection of microrobots [163]. Similarly, Contera and his team

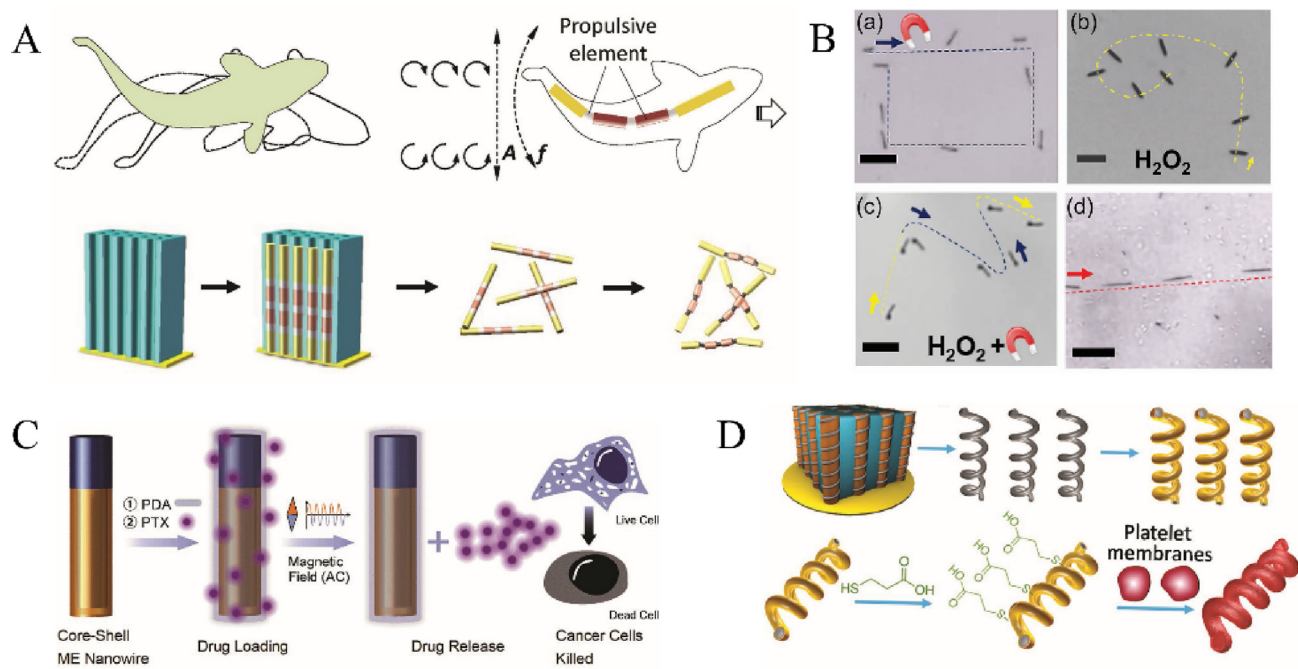


Fig. 11. Template-assisted electrochemical deposition method for preparing microrobots. A) Motion principle and preparation method of the fish-shaped microrobot. Reproduced from Reference [149] with permission from Wiley-VCH Verlag. B) Multiple actuation methods of microrobots. (a) Magnetic field push (b) Bubble push (c) Magnetic field plus bubble push (d) Acoustic actuation. Reproduced from Reference [150] with permission from Wiley-VCH Verlag. C) Applying an alternating magnetic field to control the selective release of PTX. Reproduced from Reference [157] with permission from Wiley-Blackwell. D) Microrobot wrapping platelet membrane. Reproduced from Reference [151] with permission from Wiley-Blackwell.

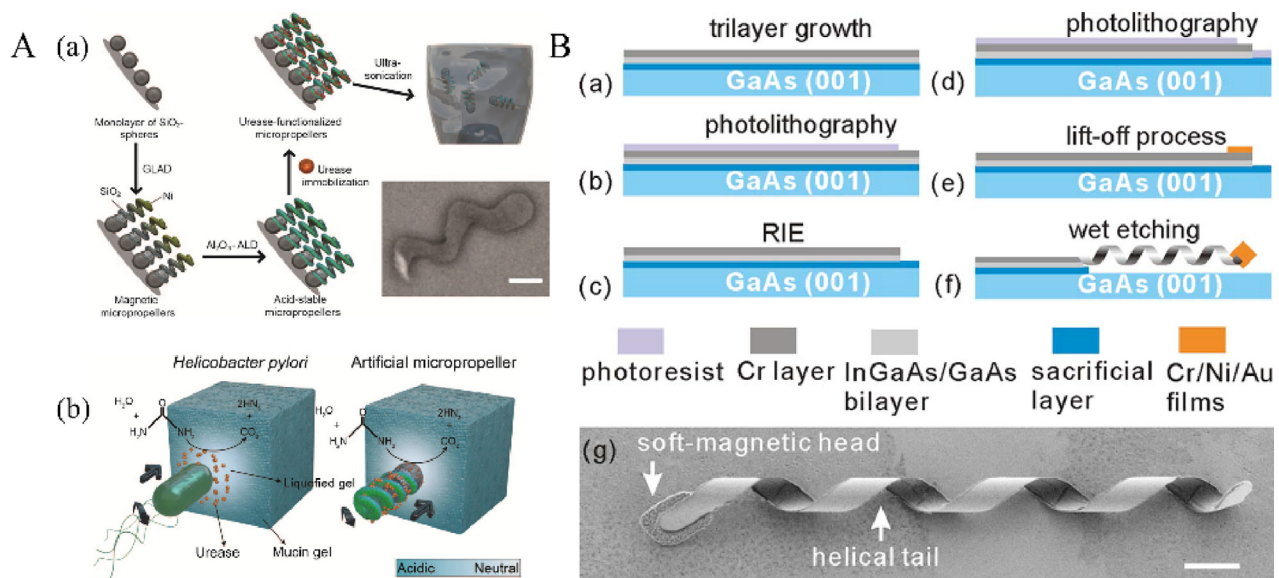


Fig. 12. An (a) Schematic diagram of the GLAD method for preparing microrobots. (b) Changes of local pH by microrobots. Reproduced from Reference [154] with permission from the American Association for the Advancement of Science. B) (a)-(f) Schematic diagram of the microrobots prepared by self-scrolling technique; (g) FESEM image of the microrobot. Reproduced from Reference [159] with permission from the American Institute of Physics.

members fabricated anisotropic microellipsoids and applied a static magnetic field of 0.25 T during the fabrication process to achieve different orientations of Fe_3O_4 nanowires. Compared with conventional commercial spherical particles, MicroEllipsoids can be better magnetically controlled under a low magnetic field intensity (≈ 10 mT) [21].

5. Application of magnetically driven microrobots

After decades of development, various forms of microrobots have been developed and microrobots can be controlled remotely, wirelessly, and precisely through the magnetic field. Low magnetic field strength is considered harmless to the human body, and

microrobots driven by magnetic fields have been used in biomedical research, for instance, cargo delivery [96,168], targeted therapy, cell manipulation, minimally invasive surgery, etc. However, when studying in vivo, the complex microenvironment in the body must be considered, and there is an immune system in the body. How to prevent the microrobot from being recognized by the immune system is also key research content. The use of micro-robots can achieve precise assembly and provide solutions for operations under special environmental requirements. Researchers have extensively studied the control of a single microrobot, but the control of the group is still in the preliminary stage. In this part, we briefly summarize the group control and selective control of the microrobot.

5.1. Biomedical applications

The application of microrobots in biomedicine is considered to be the most promising application. It can fundamentally improve the existing medical level and realize the diagnosis more efficiently. Among many applications, cargo transportation has been realized [169,170]. The research has been used in internal endoscopy and other inspections, which lays the foundation for the application in deep tissue in the future.

5.1.1. Cargo transportation

The transportation of cargo is often associated with targeted therapy, and the number of cargo loaded can be increased by increasing the specific surface area [171]. For traditional drug treatments including oral administration and injection, drugs reach the lesion through the circulatory system to exert their effects. When drugs need to be delivered through a biological barrier, traditional methods usually cause the drug to be released instantly [172]. Meanwhile, the concentration of drugs in the body increases instantly, which is easy to cause side effects. So it is difficult to achieve sustained and controlled release of drugs. With the research on microrobots in drug loading, transportation, and release, they have been widely used in drug transportation

research [173]. Microrobots encapsulated with the drugs can release the drug in control, which can improve the efficacy of drugs and reduce the damage of drugs to the human body. As shown in Fig. 13A, Chen et al. made two types of double-layer microrobots (TDMs), thumbtack-like and frisbee-like microrobots to study oral microrobots for colorectal cancer drug delivery. The outer part is composed of calcium alginate hydrogel, the inner core is chitosan microspheres loaded with drugs, and the inner Fe_3O_4 particles provide magnetic properties. Calcium alginate can remain stable in an acidic environment, which will ensure that the microrobot can reach the intestine. Calcium alginate is slowly dissolved in the alkaline environment of the gut, the chitosan spheres inside the TDMs are released, and DOX is released by Fick diffusion. The experiment proved that the drug was released continuously for ten days [174]. Through the dehydration/rehydration process, the loading of the macromolecule fluorescein isothiocyanate labeled bovine serum albumin (FITC-BSA) and the small molecule FITC are realized. With the degradation of MSPs and concentration-based diffusion, the loaded material is released. However, studies have found that at low temperatures (4°C), biological macromolecules are difficult to release through diffusion. This is attributed to the resistance generated by the cytoplasmic matrix that hinders the diffusion of macromolecules. At the same time, it was found that controlling the thickness of the Fe_3O_4 coating can affect the degradation rate of MSPs can then control the release rate of molecules [175], as shown in Fig. 13B.

The use of microrobots for drug delivery in the body usually adopts a passive method, which will lead to a decrease in delivery efficiency. The combination of a magnetic field and other fields can improve the efficiency of drug delivery. Bozuyuk et al. used a rotating magnetic field to drive double helix cones to transport DOX. Through light stimulation, 60 % of DOX can be released within 5 min, and the drug release can be terminated by light induction. It is worth noting that the spiral microcone is manufactured by methacrylamide chitosan (ChMA). The lysozyme in the body can be used to achieve the degradation of the structure. As shown in Fig. 13C, under the action of different concentrations of lysozyme,

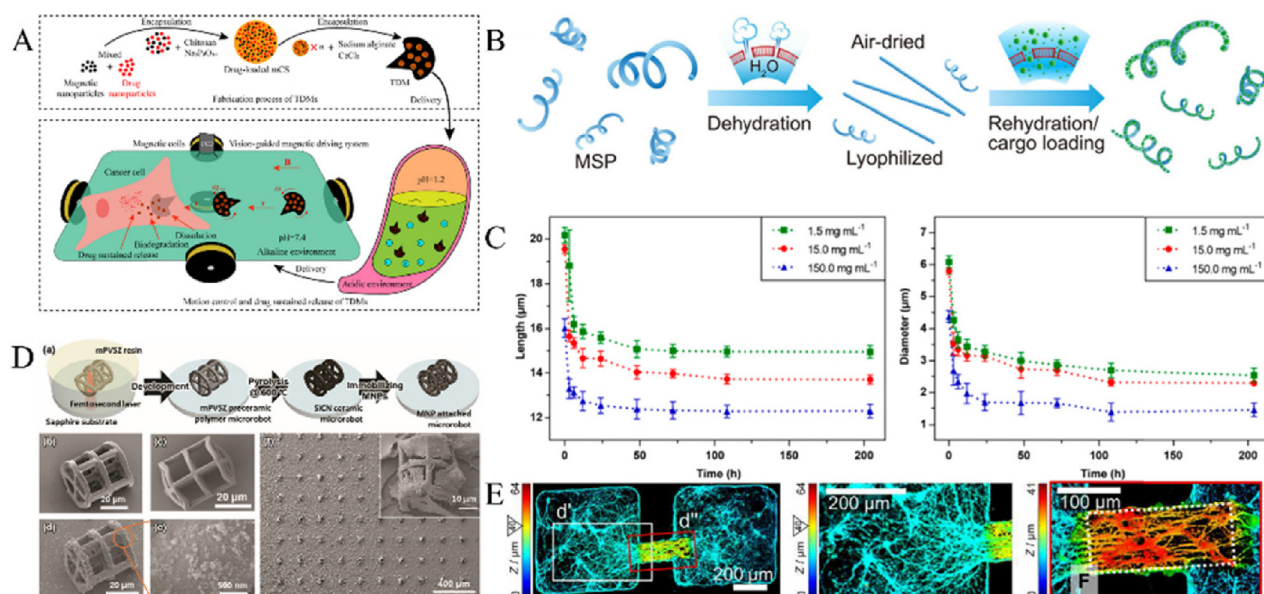


Fig. 13. Microrobots for cargo transportation. A) Schematic diagram of the manufacture, control, and drug release of microrobot TDMs. Reproduced from Reference [174] with permission from Elsevier BV. B) Using microrobots to load large molecules FITC-BSA and small molecules FITC. Reproduced from Reference [175] with permission from Elsevier BV. C) Size changes of microrobots under lysozyme degradation. Reproduced from Reference [176] with permission from the American Chemical Society. D) (a) Schematic diagram of microrobot manufacturing (b)-(f) Using microrobots to cultivate fibroblasts. Reproduced from Reference [177] with permission from John Wiley and Sons Ltd. E) Using microrobots to build bridges to realize the connection of nerve clusters. Reproduced from Reference [4] with permission from the American Association for the Advancement of Science.

the size of the microrobot was changed, and the degradation products were subjected to biocompatibility experiments with the SKBR3 breast cancer cell line. The results showed that the degradation products were not cytotoxic, and the biocompatibility of the degradation products was verified [176]. Photodynamic therapy (PDT) has been approved by the U.S. Food and Drug Administration (FDA) for the treatment of cancer, but the lack of ability to target tumor cells limits its further development. Zhang et al. created a hybrid microrobot called ISP-NMs containing iron oxide nanoparticles (IONPs), which can help improve the targeting ability of cancer cells by applying an external magnetic field. And IONPs can decompose the H_2O_2 produced by cancer cells, and provide bubble propulsion for the microrobot [178]. To improve biocompatibility, as shown in Fig. 13D, Gyak manufactured a silicon carbonitride (SiCN) ceramic microrobot, which is used to transport fibroblasts and is loaded with fibroblasts under the action of a rotating magnetic field. The average moving speed is 30 $\mu m/s$ [177]. Kim et al. created a microrobot for the cultivation and delivery of neuronal cells. In vitro experiment, as shown in Fig. 13E, a bridge was built to connect the disconnected nerve clusters. Nerve processes were found to grow around and on both sides of the nerve clusters, forming an active neural network [4]. The microrobot prepared by Lee et al. delivers drugs DOX to a designated location. Under the action of external stimulation (NIR) and dithiothreitol, magnetic nanoparticles are infused from the microrobot and collected by external electromagnetic fields, reducing the damage to the human body [179]. Xie et al. prepared hydrogel-based child-parent microrobots (CPMs) to enable microrobots carrying drugs to better reach the small intestine. External CPMs resist the attack of stomach acid and upon reaching the small intestine break down under the action of intestinal fluid. Child microrobots (CMs) release the drug at the designated site [180]. Cargo transportation is one of the important applications of micro robots, especially in the biomedical field [172]. When applied to the human body, the biocompatibility of microrobots should be considered first, and then the recycling of microrobots should be considered [176]. Although a great deal of research has been done, further research is needed in the future to improve the loading capacity and transport efficiency of microrobots. When targeted therapy is applied *in vivo*, it is necessary to further study the surface modification of microrobots in the future [173], to improve the targeting ability and then improve the drug delivery efficiency.

5.1.2. Minimally invasive surgery

Under the control of a magnetic field, the microrobot can reach areas that cannot or are not easily reached by traditional

treatment methods [181,182]. As shown in Fig. 14A, Jin et al. manufactured a micrograbber for cell capture and successfully captured single or several cells using this device. Using the thermal response characteristics of the microrobot to stretch the clamp when the temperature is low. When the trigger temperature of 37 °C is reached, the clamp starts to close [183]. For wireless drive grippers, Ghosh has done special research earlier [184]. Blockage of blood vessels in blood vessels will endanger people's health, lead to hemiplegia, and even threaten lives. Kim et al. created a microrobot with crawling and drilling capabilities. By changing the amplitude, frequency, and precessional angle, the conversion between rolling and drilling can be realized, which provides a solution for the elimination of blood clots in the body [185]. Jeong et al. developed an intravascular therapeutic microrobot system (ITMS). This system is used to drive the microrobots to move in the abdominal and iliac arteries of the living pigs, and the microrobots are controlled by twisting and hammering. It successfully penetrated the artificial thrombosis in the iliac artery, which provided a valuable preclinical test for the removal of thrombosis in the blood vessel [181]. To improve the efficiency of tumor treatment, Choi et al. combined X-ray and MRI tracking microrobots. Controlling microrobots to clog tumor blood vessels and inhibit tumor development through targeted vessel embolization and drug delivery [182]. Also for cancer treatment, Schuerle et al. used a rotating magnetic field to control the microrobot to enter tumor cells and cross the vascular barrier. In the mouse experiment, the penetration effect of the microrobot was improved by 2.16 times, which improved the effect of tumor treatment [34]. Zhang Li's team engineered the magnetic micro-driller system for Primary acquired nasolacrimal duct obstruction. The microrobot, controlled by an external electromagnet, leads to clear obstructed nasolacrimal duct (NLD), reducing patient's pain and improving safety [186]. Kim et al. prepared the guide-wired helical microrobot with a diameter of 0.125 mm, which was also used to remove the blockage in blood vessels [187].

To sum up, using a microrobot can reach areas that are difficult to reach by traditional surgery, and minimally invasive surgery by a microrobot can minimize the damage to the patient's body [181,182]. However, at present, most studies are still carried out in vitro or animals [188]. In the face of the complex human environment, it is still necessary to increase the research on microrobots in the future, improve their mobility in the human environment, and design the recycling scheme for microrobots [186].

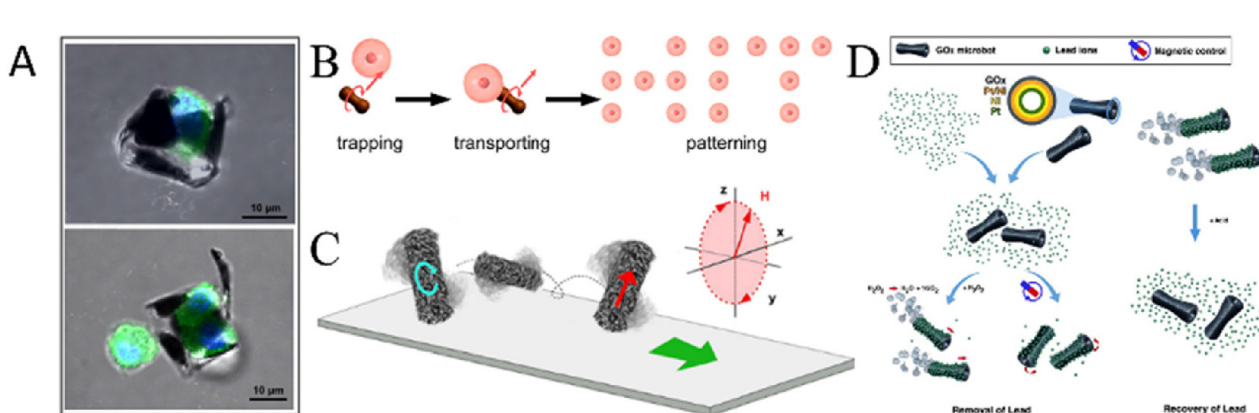


Fig. 14. A) Microrobot captures fibroblasts. Reproduced from Reference [183] with permission from the American Chemical Society. B) The microrobot moves the cells in the shape of "HIT" on the PDMS. Reproduced from Reference [189] with permission from the American Chemical Society. C) The movement posture of NR in water and solid surface. Reproduced from Reference [193] with permission from the American Chemical Society. D) Schematic diagram of pollutant removal and self-recovery of GOx-microrobot. Reproduced from Reference [191] with permission from the American Chemical Society.

5.1.3. Cell manipulation

The effective miniaturization of the machine completes the manipulation of the size and scale of a single cell. With further research on microscopic operations, researchers have now achieved cell separation and patterning operations by manipulating single cells, which will be beneficial to drug development and cell analysis. Lin et al. created a peanut-shaped microrobot for cell manipulation. The microrobot can perform rolling and swinging motions under the action of a rotating magnetic field and a cone-shaped rotating magnetic field. The maximum forward speed can reach $10.6 \mu\text{m/s}$ in rolling mode, and $14.5 \mu\text{m/s}$ in swing mode. And by combining the two motion modes, the capture, transportation, and release of NIH 3 T3 cells are realized. It is particularly noteworthy that the transportation of cells is achieved through noncontact methods, which will reduce the impact on the cell body during the transportation process. As shown in Fig. 14B, the control of using microrobots to transport 15 cells to the PDMS board shows the pattern of HIT [189]. After in vitro fertilization, the embryos (zygotes) need to be transferred back to the fallopian tube, and then enter the uterus to achieve embryo development. The use of this microrobot does not require external light, heat, and other stimuli, and can capture, transport, and release cells only through magnetically induced rotation [190]. Pumera et al. prepared a curved microrobot and used it as a scalpel to operate on a single cancer cell, using a rotating magnetic field to drive the microrobot into the cytoplasm of the cancer cell and extract cell debris. The plasma membrane of the cell remained intact during the entire process [8]. By controlling the microrobot, the manipulation of cells can be realized by contact or noncontact method. To reduce the damage to cells, the noncontact method is the main research direction in the future [189]. It is necessary to further study the movement mode of micro robots, study the mechanical relationship between microrobots and cells in a liquid environment, and improve the control precision of microrobots to cells [190].

5.2. Removal of toxic and harmful substances in the environment

With the rapid development of the world's industrialization, industrial by-products contain a large number of toxic and hazardous substances, and heavy metals are also discharged into the natural environment along with wastewater. How to remove them effectively has been widely concerned by researchers [191,192]. García-Torres et al. manufactured magnetic mesoporous CoNi@Pt NRs (magnetic nanorods) with a core-shell structure. As shown in Fig. 14C, the Pt shell catalyzes the borohydride, promotes the hydrolysis of the borohydride, and achieves the degradation of pollutants. The generated H_2 promotes the movement of NRs [193]. Vilela manufactures graphene oxide-based microbots (GOx-microbots), as shown in Fig. 14D, to achieve the capture, transfer, and removal of heavy metal lead in the environment. Under the action of an external magnetic field, after 60 min of purification, the concentration dropped from 1000 ppb to less than 50 ppb [191]. The development of the petrochemical industry has brought tremendous changes to human life, but the leakage of oil pollution and plastic particles has also caused harm to the environment. Sun et al. fabricated a microrobot with porous burrs. The average diameter is $30 \pm 0.04 \mu\text{m}$, and the surface has hydrophobic and lipophilic properties. Under the action of different rotating magnetic fields, three modes of motion, rolling, rotating, and swinging can be realized, and the removal of oil and plastic particles can be achieved through individual or group control [194]. Mushtaq et al. fabricated tubular and spiral nanorobots to achieve the degradation of pollutants. Within 6 h, the degradation efficiency of pollutant RhB can reach 90 % [192]. To improve detection capability, Pumera et al. prepared MagRobot@anti-SARS-CoV-2 SP and Ag-AuNRs@anti-SARS-CoV-2 SP. The SARS-CoV-2 virus was collected

and detected by a transverse rotating magnetic field. Under the action of collective self-assembly behavior, the detection sensitivity is improved [195]. Similarly, Ma et al. prepared rod magnetically driven nanorobots (MNRs) as immunoassay probes for ELLSA analysis. Self-made detection unit with three wells. When PCT was selected as a biomarker, MNRs moved in different wells under the action of the magnetic field, and the detection line was 0.18 ng/ml , indicating good performance [196]. When using a microrobots to remove toxic and harmful substances from the environment, work efficiency is the primary consideration. At present, it is mainly through recovering or decomposing toxic and harmful substances. Because of the small size of the microrobot, to improve work efficiency, microrobot cooperation is one of the most feasible schemes. Group control and recovery of microrobots is an important part of future research.

5.3. Microoperation

Microrobots can also be used for micromanipulation, transportation and classification of microobjects, and operations. Tasoglu et al. used a $750 \mu\text{m} \times 750 \mu\text{m} \times 250 \mu\text{m}$ cube robot to perform 2D and 3D spatial movement of polystyrene beads and polydimethylsiloxane (PDMS) blocks [197], as shown in Fig. 15A. Youssefi et al. used a modified square three-axis Helmholtz coil to drive cubic microrobots with a control step length of 3 % of the body length. On the surface of the plastic Petri dish, the microrobot contacts the aluminum nut point or surface and pushes it to move directionally [198]. It is also the research on the propulsion of microstructures on the surface, in order to reduce the effect of slippage during the propulsion process, realize rolling propulsion, and increase the propulsion speed. Inspired by the smooth movement of square wheels on roads with truncated catenaries, Yang et al. created μ wheels that can shift four times faster. By constructing different pavement structures, the separation of isomeric μ wheels can be realized under the magnetic field drive, which provides a new idea for the separation of microscopic objects, as shown in Fig. 15B [199]. Using permanent magnets to drive a magnetically driven microtool (MMT) can output a force of the order of millinewtons, but it has disadvantages such as low positioning accuracy. As shown in Fig. 15C, Hagiwara et al. combined permanent magnet drive and ultrasonic drive to improve the accuracy of the operation and completed the cutting of pig oocytes in a few seconds [200].

To sum up, microrobot can control the position of materials in the microworld through microoperation, and then can realize micro-assembly [198,199], which can solve the difficult problem of traditional macro-operation. In the future, it is still necessary to improve the research on the control accuracy of microrobot [200], so as to improve the operation accuracy of micro-manipulation.

5.4. Group manipulation and selective control

So far, extensive research has been carried out on the in vivo and in vitro applications of a single microrobot. However, in order to achieve better application effects, it is necessary to control the group microrobots [201]. For instance, population control can increase the content of drug delivery and increase the speed of removing pollutants in the environment. By applying a programmed alternating magnetic field to a single type of peanut-shaped microrobot group, Xie et al. realized the formation operation of the microrobots, and can switch between the four formations of liquid, chain, vortex, and ribbon [202], as shown in Fig. 16A. Zheng et al. prepared mesoporous iron oxide microrobots, which can mechanically clear the biofilm under the action of magnetic field, and can generate three kinds of active oxygen for sterilization through chemical reaction with H_2O_2 . Under the action of the alternating magnetic field, the microrobot can generate heat,

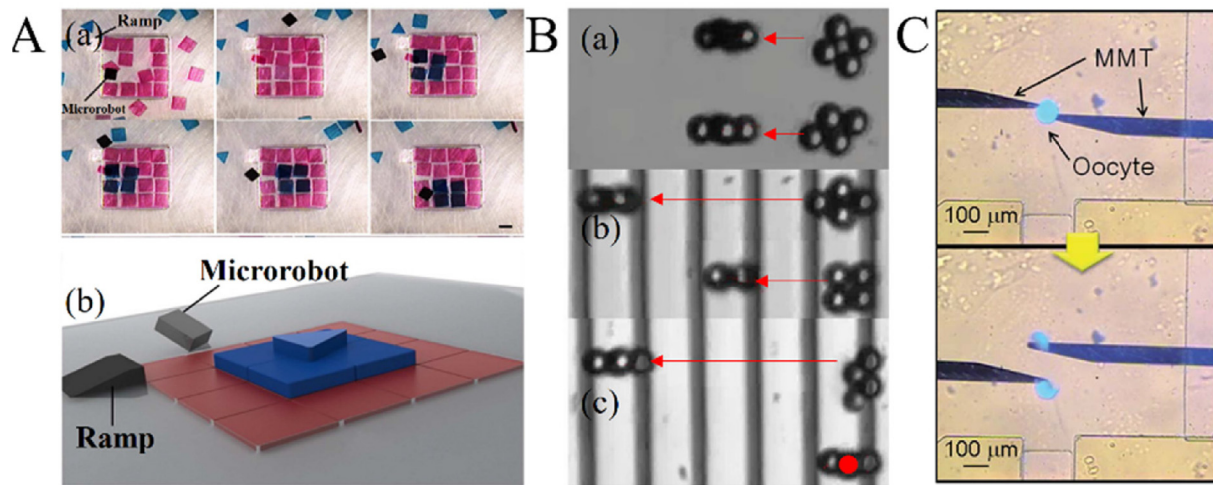


Fig. 15. Microrobots for micromanipulation. A) (a) Microrobots push objects to form a three-layer heterogeneous pyramid structure. (b) The complete structure diagram of the three-layer heterogeneous pyramid structure. Reproduced from Reference [197] with a permission from Springer Nature. B) Separation of diamond and square μ wheels. (a) Diamond and square μ wheels move the same distance on a flat surface. (b) The running distance of diamond and square μ wheels on the textured surface is different, the frequency is 1 Hz. (c) The running distance of diamond and square μ wheels on the textured surface is different, the frequency is 0.2 Hz. Reproduced from Reference [199] with a permission from American Association for the Advancement of Science. C) Using microrobots to cut the oocyte and take out the nucleus. Reproduced from Reference [200] with a permission from Royal Society of Chemistry.

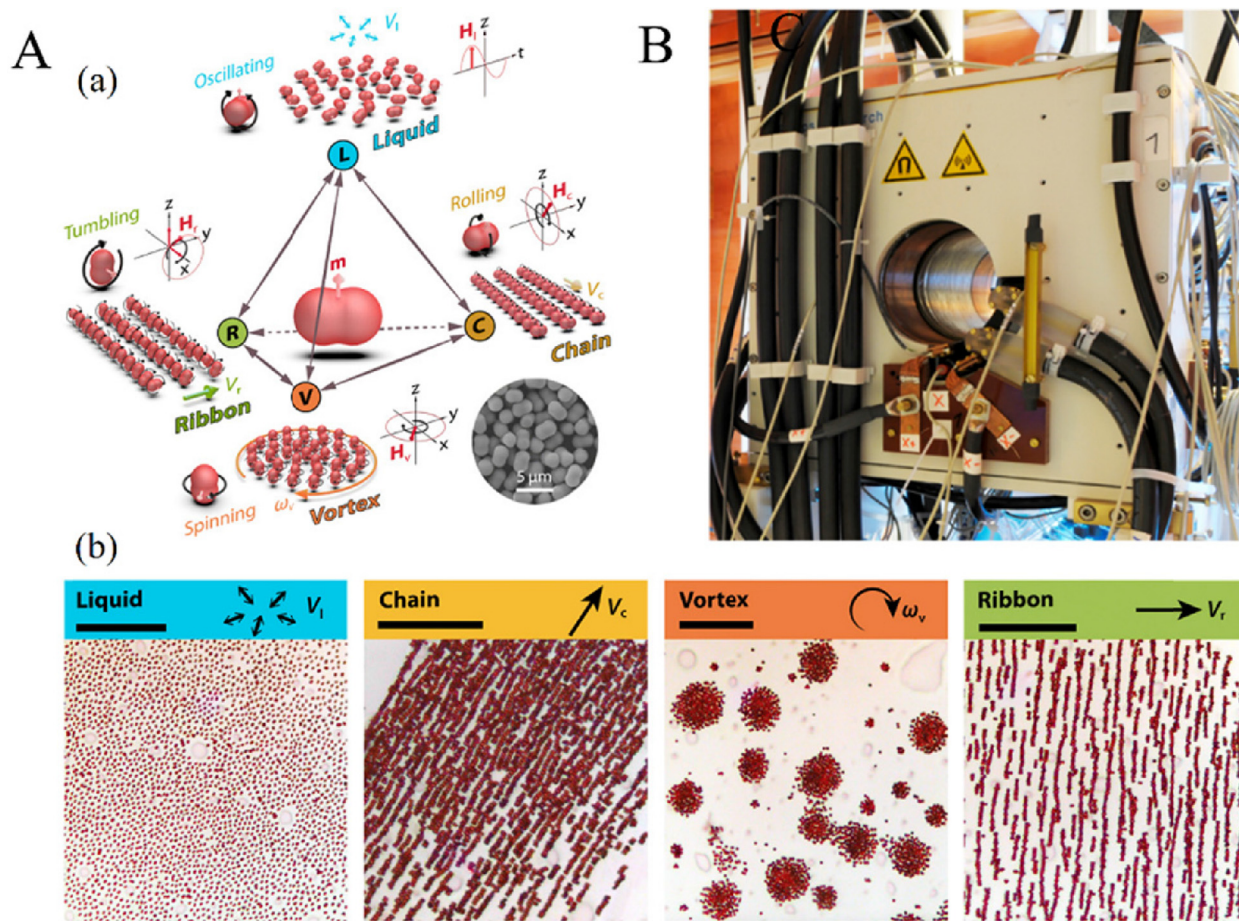


Fig. 16. A) (a) Schematic diagram of the four deformation modes of microrobots and the transformation between them. (b) From left to right are snapshots of the four movement patterns. Reproduced from Reference [202] with a permission from American Association for the Advancement of Science. B) Photo of magnetic field generator. Reproduced from Reference [204] with a permission from American Association for the Advancement of Science.

promote the generation of active oxygen, and improve the sterilization efficiency [203]. To solve the problem that it is difficult for microrobots to independently change their motion states in response to environmental changes, Zhang et al. applied deep learning to group control of microrobots. Autonomy levels of environment-adaptive microrobot swarm navigation (from L1 to L4) are proposed, which will be beneficial to realize the autonomous movement of microrobot crowd [42].

In addition to the demand for group control, how to selectively control a single or part of a group has become another important research direction. As mentioned above, it has been studied to selectively drive some microrobots in the group by applying magnetic fields of different frequencies. At a certain frequency, some microrobots can be driven and some are at rest. Group robots with different structures can be constructed. When the applied magnetic fields are different, the microrobots with different structures will react differently to the same magnetic field. For homogeneous robots, Rahmer and his researchers proposed a technique that can use magnetic fields to selectively drive individual microrobots. As shown in Fig. 16B, three groups of orthogonal coils and an iron core in the Z direction are used to form a magnetic field generator with an inner diameter of 12 cm. By applying current in the coil with the same amplitude and opposite direction, Maxwell coil is constructed. At this time, the field in the center region is zero, which is called field-free point (FFP). When the microrobot is in FFP, the magnetic field gradient is very low, and it can be manipulated by applying an external rotating magnetic field. When the FFP is shifted to other regions, other microrobots can be independently manipulated using the same method [204]. Xu et al. prepared millirobots with the same shape but different magnetization directions. Under the action of the same magnetic field, different millirobots will have different speeds. For the first time, they realized independent position control of four magnetic soft millirobots and independent path following control of three magnetic soft millirobots [45]. With the deepening of the research on microrobot, group control is the focus of current and future research. Group control can not only improve efficiency, but also achieve complex functions. A bridge between micro and macro will be constructed through group control, which can not only enhance the effect of micro field, but also realize the agglomeration effect of macro field. Similarly, it is also an important research direction to selectively control the individual in the group, which will be able to realize the individual control of the group and help the microrobot to complete special tasks.

6. Conclusion and prospective

The development and research of microrobots provide powerful tools for people's understanding and exploration of microworld. Because the magnetic field has the advantages of being harmless to the human body, convenient operation, remote wireless control, etc., it has been widely used in the manipulation of microrobots. According to different motion models, the shapes of microrobots are also various, including spiral, tubular, spherical, etc. And with the introduction of new actuation theories, various new structures have also been used in the design and manufacture of microrobots. The development of flexible materials and flexible structures provides new options for the manufacture of microrobots. For the driving of microrobots, permanent magnets and electromagnets have their advantages. Microrobots are currently mainly used in the field of biomedicine. Drug delivery, targeted therapy, and minimally invasive surgery have been extensively studied. In addition, microrobots are also used in the removal of toxic and hazardous substances in the environment, and microoperations under special working conditions. This article is to review the development of

magnetically driven microrobots in recent years, summarize the materials, methods, and applications of manufacturing microrobots, and provides research directions for related researchers.

There are still a lot of development prospects in terms of actuation, materials, and processing methods. Researchers are working to achieve large-scale rapid manufacturing of microrobots with excellent performance. The development of microrobots in the field of biomedicine has attracted the most attention. But so far, applications *in vivo* have mainly focused on endoscopy. The treatment of deep tissues is still *in vitro* simulation or animal testing. It is not yet available for large-scale human clinical trials. The first reason is the manufacture and actuation of microrobots. Secondly, the existence of a complex immune system in the human body puts forward higher requirements for the application of microrobots *in vivo*. At present, researchers have used various methods to improve biocompatibility in the process of manufacturing microrobots, including the use of natural non-toxic, and harmless microorganisms, adding biocompatible material Ti, and using red blood cells to encapsulate microrobots. But there is still a long way to go before the real large-scale application *in vivo*. The choice of materials for microrobots will largely determine the field of its application. The in-depth research of flexible materials and intelligent materials provides a new choice for the manufacturing of microrobots. This is also conducive to microrobots to achieve deformation operations in complex environments and complete tasks more efficiently. Recently, the programming operation of microrobots has also been further developed. By manufacturing various micro clamps, the target can be captured and transported, which is also conducive to the realization of customized manufacturing of microrobots. And with the in-depth research on the actuation of microrobots, crowd control, and selective control have attracted more and more attention. The use of group control can double the function effect, while selective control can achieve fine operation and achieve collaboration. The work, as stated in the article, has been preliminarily researched. In the future, further research will be carried out on the materials and structure of microrobots to better complete group control and selective operations.

In general, microrobots are an important tool for people to understand and explore microworld. Researchers have made in-depth research on magnetic driven microrobots, and have achieved important results. In the future, we need to further explore the manufacturing method and actuating principle, to achieve breakthrough progress as soon as possible.

Data availability statement

All data that support the findings of this study are included in the article.

Data availability

No data was used for the research described in the article.

Declaration of Competing Interest

The authors declare that they have no known competing financial interests or personal relationships that could have appeared to influence the work reported in this paper.

Acknowledgments

The authors wish to acknowledge the funding provided by the National Natural Science Foundation of China (Project No. 62273289) and the Joint fund of Science & Technology Department of Liaoning Province and State Key Laboratory of Robotics (Project No. 2021-KF-22-03).

References

- [1] K.T. Nguyen, H.-S. Lee, J. Kim, E. Choi, J.-O. Park, C.-S. Kim, A composite electro-permanent magnetic actuator for microrobot manipulation, *Int. J. Mech. Sci.* 229 (2022) 107516.
- [2] S.Jeon, S.H. Park, E. Kim, J.-Y. Kim, S.W. Kim, H. Choi, A Magnetically Powered Stem Cell-Based Microrobot for Minimally Invasive Stem Cell Delivery via the Intranasal Pathway in a Mouse Brain, *Adv. Healthc. Mater.* 10 (19) (2021) 2100801.
- [3] D. Gong, N. Celi, L. Xu, D. Zhang, J. Cai, CuS nanodots-loaded biohybrid magnetic helical microrobots with enhanced photothermal performance, *Mater. Today Chem.* 23 (2022) 100694.
- [4] E. Kim, S. Jeon, H.-K. An, M. Kianpour, S.-W. Yu, J.-Y. Kim, J.-C. Rah, H. Choi, A magnetically actuated microrobot for targeted neural cell delivery and selective connection of neural networks, *Science, Advances* 6 (39) (2020) eabb5696.
- [5] C. Xu, Z. Yang, G.Z. Lum, Small-Scale Magnetic Actuators with Optimal Six Degrees-of-Freedom, *Adv. Mater.* 33 (23) (2021) 2100170.
- [6] C. Xin, D. Jin, Y. Hu, L. Yang, R. Li, L. Wang, Z. Ren, D. Wang, S. Ji, K. Hu, D. Pan, H. Wu, W. Zhu, Z. Shen, Y. Wang, J. Li, L. Zhang, D. Wu, J. Chu, Environmentally Adaptive Shape-Morphing Microrobots for Localized Cancer Cell Treatment, *ACS Nano* 15 (11) (2021) 18048–18059.
- [7] S. Lee, S. Lee, S. Kim, C.-H. Yoon, H.-J. Park, J.-Y. Kim, H. Choi, Fabrication and Characterization of a Magnetic Drilling Actuator for Navigation in a Three-dimensional Phantom Vascular Network, *Sci. Rep.* 8 (1) (2018) 3691.
- [8] J. Vyskočil, C.C. Mayorga-Martinez, E. Jablonská, F. Novotný, T. Rumí, M. Pumera, Cancer Cells Microsurgery via Asymmetric Bent Surface Au/Ag/Ni Microrobotic Scalpels Through a Transversal Rotating Magnetic Field, *ACS Nano* 14 (7) (2020) 8247–8256.
- [9] T. Bhuyan, A.T. Simon, S. Maity, A.K. Singh, S.S. Ghosh, D. Bandyopadhyay, Magnetotactic T-Budbots to Kill-n-Clean Biofilms, *ACS Appl. Mater. Interfaces* 12 (39) (2020) 43352–43364.
- [10] D. Loganathan, C.-L. Hsieh, B.-E. Shi, Y.-H. Lu, C.-Y. Chen, An On-Demand Microrobot with Building Block Design for Flow Manipulation, *Advanced Materials Technologies* n/a(n/a) (2022) 2201073.
- [11] A.K. Singh, T. Bhuyan, S. Maity, T.K. Mandal, D. Bandyopadhyay, Magnetically Actuated Carbon Soot Nanoparticle-Based Catalytic CARBOts Coated with Ni/Pt Nanofilms for Water Detoxification and Oil-Spill Recovery, *ACS Appl. Nano Mater.* 3 (4) (2020) 3459–3470.
- [12] R. Maria-Hormigos, C.C. Mayorga-Martinez, M. Pumera, Soft Magnetic Microrobots for Photoactive Pollutant Removal, *Small Methods* n/a(n/a) (2022) 2201014.
- [13] X. Wang, D. Lin, Y. Zhou, N. Jiao, S. Tung, L. Liu, Multistimuli-Responsive Hydroplaning Superhydrophobic Microrobots with Programmable Motion and Multifunctional Applications, *ACS Nano* 16 (9) (2022) 14895–14906.
- [14] J. Li, F. Ji, D.H.L. Ng, J. Liu, X. Bing, P. Wang, Bioinspired Pt-free molecularly imprinted hydrogel-based magnetic Janus micromotors for temperature-responsive recognition and adsorption of erythromycin in water, *Chem. Eng. J.* 369 (2019) 611–620.
- [15] T. Maric, M.Z.M. Nasir, N.F. Rosli, M. Budanović, R.D. Webster, N.-J. Cho, M. Pumera, Microrobots Derived from Variety Plant Pollen Grains for Efficient Environmental Clean Up and as an Anti-Cancer Drug Carrier, *Adv. Funct. Mater.* 30 (19) (2020) 2000112.
- [16] B. Jurado-Sánchez, M. Pacheco, J. Rojo, A. Escarpa, Magnetocatalytic Graphene Quantum Dots Janus Micromotors for Bacterial Endotoxin Detection, *Angew. Chem. Int. Ed.* 56 (24) (2017) 6957–6961.
- [17] E. Kopperger, J. List, S. Madhira, F. Rothfischer, D.C. Lamb, F.C. Simmel, A self-assembled nanoscale robotic arm controlled by electric fields, *Science* 359 (6373) (2018) 296.
- [18] G. Go, V.D. Nguyen, Z. Jin, J.-O. Park, S. Park, A Thermo-electromagnetically Actuated Microrobot for the Targeted Transport of Therapeutic Agents, *Int. J. Control. Autom. Syst.* 16 (3) (2018) 1341–1354.
- [19] Y. Dong, L. Wang, K. Yuan, F. Ji, J. Gao, Z. Zhang, X. Du, Y. Tian, Q. Wang, L. Zhang, Magnetic Microswarm Composed of Porous Nanocatalysts for Targeted Elimination of Biofilm Occlusion, *ACS Nano* 15 (3) (2021) 5056–5067.
- [20] Q. Wang, L. Yang, J. Yu, L. Zhang, Characterizing dynamic behaviors of three-particle paramagnetic microswimmer near a solid surface, *Robot. Biomim.* 4 (1) (2017) 20.
- [21] A. Bonilla-Brunner, I. Llorente García, B. Jang, M. Amano Patiño, V. Alimchandani, B.J. Nelson, S. Pané, S. Contera, Polymeric microellipsoids with programmed magnetic anisotropy for controlled rotation using low (≈ 10 mT) magnetic fields, *Applied. Mater. Today* 18 (2020) 100511.
- [22] L. Xie, X. Pang, X. Yan, Q. Dai, H. Lin, J. Ye, Y. Cheng, Q. Zhao, X. Ma, X. Zhang, G. Liu, X. Chen, Photoacoustic Imaging-Trackable Magnetic Microswimmers for Pathogenic Bacterial Infection Treatment, *ACS Nano* 14 (3) (2020) 2880–2893.
- [23] R. Maria-Hormigos, C.C. Mayorga-Martinez, M. Pumera, Magnetic Hydrogel Microrobots as Insecticide Carriers for In Vivo Insect Pest Control in Plants, *Small* n/a(n/a) (2022) 2204887.
- [24] K. Villa, M. Pumera, Fuel-free light-driven micro/nanomachines: artificial active matter mimicking nature, *Chem. Soc. Rev.* 48 (19) (2019) 4966–4978.
- [25] M. Sun, W. Chen, X. Fan, C. Tian, L. Sun, H. Xie, Cooperative recyclable magnetic microsubmarines for oil and microplastics removal from water, *Appl. Mater. Today* 20 (2020) 100682.
- [26] T. Maric, M.Z.M. Nasir, M. Budanovic, O. Alduhaish, R.D. Webster, M. Pumera, Corrosion of light powered Pt/TiO₂ microrobots, *Appl. Mater. Today* 20 (2020) 100659.
- [27] M. Valdez-Garduño, M. Leal-Estrada, E.S. Oliveros-Mata, D.I. Sandoval-Bojorquez, F. Soto, J. Wang, V. García-Gradilla, Density Asymmetry Driven Propulsion of Ultrasound-Powered Janus Micromotors, *Adv. Funct. Mater.* 30 (50) (2020) 2004043.
- [28] Z. Li, L. Bai, C. Zhou, X. Yan, L. Mair, A. Zhang, L. Zhang, W. Wang, Highly Acid-Resistant, Magnetically Steerable Acoustic Micromotors Prepared by Coating Gold Microrods with Fe₃O₄ Nanoparticles via pH Adjustment, *Part. Part. Syst. Char.* 34 (2) (2017) 1600277.
- [29] S. Mohanty, A. Paul, P.M. Matos, J. Zhang, J. Sikorski, S. Misra, CeFlowBot: A Biomimetic Flow-Driven Microrobot that Navigates under Magneto-Acoustic Fields, *Small* 18 (9) (2022) 2105829.
- [30] M. Li, J. Wu, D. Lin, J. Yang, N. Jiao, Y. Wang, L. Liu, A diatom-based biohybrid microrobot with a high drug-loading capacity and pH-sensitive drug release for target therapy, *Acta Biomater.* 154 (2022) 443–453.
- [31] A. Terzopoulou, M. Palacios-Corella, C. Franco, S. Sevim, T. Dysli, F. Mushtaq, M. Romero-Angel, C. Martí-Gastaldo, D. Gong, J. Cai, X.-Z. Chen, M. Pumera, A. J. deMello, B.J. Nelson, S. Pané, J. Puigmarti-Luis, Biотemplating of Metal-Organic Framework Nanocrystals for Applications in Small-Scale Robotics, *Adv. Funct. Mater.* 32 (13) (2022) 2107421.
- [32] V. de la Asunción-Nadal, C. Franco, A. Veciana, S. Ning, A. Terzopoulou, S. Sevim, X.-Z. Chen, D. Gong, J. Cai, P.D. Wendel-Garcia, B. Jurado-Sánchez, A. Escarpa, J. Puigmarti-Luis, S. Pané, MoSBOTs: Magnetically Driven Biотemplated MoS₂-Based Microrobots for Biomedical Applications, *Small* 18 (33) (2022) 2203821.
- [33] Z. Zheng, H. Wang, S.O. Demir, Q. Huang, T. Fukuda, M. Sitti, Programmable aniso-electrodeposited modular hydrogel microrobots, *Science Advances* 8 (50) eade6135.
- [34] T. Gwisai, N. Mirkhani, M.G. Christiansen, T.T. Nguyen, V. Ling, S. Schuerle, Magnetic torque-driven living microrobots for increased tumor infiltration, *Science Robotics* 7(71) eabo0665.
- [35] C.C. Mayorga-Martinez, J. Zelenka, K. Klíma, P. Mayorga-Burrezo, L. Hoang, T. Rumí, M. Pumera, Swarming Magnetic Photoactive Microrobots for Dental Implant Biofilm Eradication, *ACS Nano* 16 (6) (2022) 8694–8703.
- [36] E. Lauga, T.R. Powers, The hydrodynamics of swimming microorganisms, *Rep. Prog. Phys.* 72 (9) (2009) 096601.
- [37] E.M. Purcell, Life at low Reynolds number, *Am. J. Phys.* 45 (1) (1977) 3–11.
- [38] D. Zhong, W. Li, Y. Qi, J. He, M. Zhou, Photosynthetic Biohybrid Nanoswimmers System to Alleviate Tumor Hypoxia for FL/PA/MR Imaging-Guided Enhanced Radio-Photodynamic Synergetic Therapy, *Adv. Funct. Mater.* 30 (17) (2020) 1910395.
- [39] V. Magdanz, I.S.M. Khalil, J. Simmchen, G.P. Furtado, S. Mohanty, J. Gebauer, H. Xu, A. Klingner, A. Aziz, M. Medina-Sánchez, O.G. Schmidt, S. Misra, IRONSperm: Sperm-templated soft magnetic microrobots, *Science, Advances* 6 (28) (2020) eaba5855.
- [40] H. Xu, M. Medina-Sánchez, M.F. Maitz, C. Werner, O.G. Schmidt, Sperm Micromotors for Cargo Delivery through Flowing Blood, *ACS Nano* 14 (3) (2020) 2982–2993.
- [41] Q. Wang, K.F. Chan, K. Schweizer, X. Du, D. Jin, S.C.H. Yu, B.J. Nelson, L. Zhang, Ultrasound Doppler-guided real-time navigation of a magnetic microswarm for active endovascular delivery, *Science, Advances* 7 (9) (2021) eabe5914.
- [42] L. Yang, J. Jiang, X. Gao, Q. Wang, Q. Dou, L. Zhang, Autonomous environment-adaptive microrobot swarm navigation enabled by deep learning-based real-time distribution planning, *Nat. Machine Intell.* 4 (5) (2022) 480–493.
- [43] X. Dong, M. Sitti, Controlling two-dimensional collective formation and cooperative behavior of magnetic microrobot swarms, *Int. J. Robot. Res.* 39 (5) (2020) 617–638.
- [44] R. Khalesi, H. Nejat Pishkenari, G. Vossoughi, Independent control of multiple magnetic microrobots: design, dynamic modelling, and control., *J. Micro-Bio Robot.* 16 (2) (2020) 215–224.
- [45] T. Xu, C. Huang, Z. Lai, X. Wu, Independent Control Strategy of Multiple Magnetic Flexible Millirobots for Position Control and Path Following, *IEEE Trans. Rob.* 38 (5) (2022) 2875–2887.
- [46] Z. Wu, Y. Chen, D. Mukasa, O.S. Pak, W. Gao, Medical micro/nanorobots in complex media, *Chem. Soc. Rev.* 49 (22) (2020) 8088–8112.
- [47] Y. Zhang, K. Yuan, L. Zhang, Micro/Nanomachines: from Functionalization to Sensing and Removal, *Adv. Mater. Technol.* 4 (4) (2019) 1800636.
- [48] G. Adam, S. Chowdhury, M. Guix, B.V. Johnson, C. Bi, D. Cappelleri, Towards Functional Mobile Microrobotic Systems, *Robotics* 8 (3) (2019).
- [49] S.Y. Hann, H. Cui, M. Nowicki, L.G. Zhang, 4D printing soft robotics for biomedical applications, *Addit. Manuf.* 36 (2020) 101567.
- [50] B. Wang, K. Kostarelos, B.J. Nelson, L. Zhang, Trends in Micro-/Nanorobotics: Materials Development, Actuation, Localization, and System Integration for Biomedical Applications, *Adv. Mater.* 33 (4) (2021) 2002047.
- [51] J. Puigmarti-Luis, E. Pellicer, B. Jang, G. Chatzipirpiridis, S. Sevim, X.-Z. Chen, B. J. Nelson, S. Pané, 26 - Magnetically and chemically propelled nanowire-based swimmers, in: M. Vázquez (Ed.), *Magnetic Nano- and Microwires*, (Second Edition), Woodhead Publishing, 2020, pp. 777–799.
- [52] M.P. Kummer, J.J. Abbott, B.E. Kratochvil, R. Borer, A. Sengul, B.J. Nelson, OctoMag: An Electromagnetic System for 5-DOF Wireless Micromanipulation, *IEEE Trans. Rob.* 26 (6) (2010) 1006–1017.
- [53] I.S.M. Khalil, B.E. Wissa, B.G. Salama, S. Stramigoli, Wireless motion control of paramagnetic microparticles using a magnetic-based robotic system with an open-configuration, 2015 International Conference on Manipulation,

- Manufacturing and Measurement on the Nanoscale (3M-NANO), 2015, pp. 190–196.
- [54] X. Xu, S. Hou, N. Wattanatorn, F. Wang, Q. Yang, C. Zhao, X. Yu, H.-R. Tseng, S.J. Jonas, P.S. Weiss, Precision-Guided Nanospears for Targeted and High-Throughput Intracellular Gene Delivery, *ACS Nano* 12 (5) (2018) 4503–4511.
- [55] M. Yousef, H. Nejat Pishkenari, Independent position control of two identical magnetic microrobots in a plane using rotating permanent magnets., *J. Micro-Bio Robotics* 17 (1) (2021) 59–67.
- [56] S. Zhang, M. Yin, Z. Lai, C. Huang, C. Wang, W. Shang, X. Wu, Y. Zhang, T. Xu, Design and Characteristics of 3D Magnetically Steerable Guidewire System for Minimally Invasive Surgery, *IEEE Rob. Autom. Lett.* 7 (2) (2022) 4040–4046.
- [57] A. Zarrouk, K. Belharet, O. Tahri, Vision-based magnetic actuator positioning for wireless control of microrobots, *Rob. Auton. Syst.* 124 (2020) 103366.
- [58] X. Bai, D. Chen, W. Zhang, H. Ossian, Y. Chen, Y. Feng, L. Feng, F. Arai, Magnetically Driven Bionic Millirobots with a Low-Delay Automated Actuation System for Bioparticles Manipulation, *Micromachines* 11 (2) (2020).
- [59] I.S.M. Khalil, A. Alfar, A.F. Tabak, A. Klingner, S. Stramigioli, M. Sitti, Positioning of drug carriers using permanent magnet-based robotic system in three-dimensional space, *IEEE International Conference on Advanced Intelligent Mechatronics (AIM) 2017* (2017) 1117–1122.
- [60] A.W. Mahoney, J.J. Abbott, Generating Rotating Magnetic Fields With a Single Permanent Magnet for Propulsion of Untethered Magnetic Devices in a Lumen, *IEEE Trans. Rob.* 30 (2) (2014) 411–420.
- [61] F. Qiu, L. Zhang, K.E. Peyer, M. Casarosa, A. Franco-Obregón, H. Choi, B.J. Nelson, Noncytotoxic artificial bacterial flagella fabricated from biocompatible ORMOCOMP and iron coating, *J. Mater. Chem. B* 2 (4) (2014) 357–362.
- [62] C. Chen, L. Chen, P. Wang, L.-F. Wu, T. Song, Steering of magnetotactic bacterial microrobots by focusing magnetic field for targeted pathogen killing, *J. Magn. Magn. Mater.* 479 (2019) 74–83.
- [63] D. Byun, J. Choi, K. Cha, J.-O. Park, S. Park, Swimming microrobot actuated by two pairs of Helmholtz coils system, *Mechatronics* 21 (1) (2011) 357–364.
- [64] S. Yu, N. Ma, H. Yu, H. Sun, X. Chang, Z. Wu, J. Deng, S. Zhao, W. Wang, G. Zhang, W. Zhang, Q. Zhao, T. Li, Self-Propelled Janus Microrobots Swimmers under a Rotating Magnetic Field, *Nanomaterials* 9 (12) (2019).
- [65] Q. Fu, S. Guo, S. Zhang, H. Hirata, H. Ishihara, Characteristic Evaluation of a Shrouded Propeller Mechanism for a Magnetic Actuated Microrobot, *Micromachines* 6 (9) (2015).
- [66] Q. Fu, S. Zhang, S. Guo, J. Guo, Performance Evaluation of a Magnetically Actuated Capsule Microrobotic System for Medical Applications, *Micromachines* 9 (12) (2018).
- [67] J.O. Kwon, J.S. Yang, J.B. Chae, S.K. Chung, Micro-object manipulation in a microfabricated channel using an electromagnetically driven microrobot with an acoustically oscillating bubble, *Sens. Actuators, A* 215 (2014) 77–82.
- [68] S. Jeong, H. Choi, K. Cha, J. Li, J.-O. Park, S. Park, Enhanced locomotive and drilling microrobot using precessional and gradient magnetic field, *Sens. Actuators, A* 171 (2) (2011) 429–435.
- [69] S.M. Jeon, G.H. Jang, H.C. Choi, S.H. Park, J.O. Park, Magnetic navigation system for the precise helical and translational motions of a microrobot in human blood vessels, *J. Appl. Phys.* 111 (7) (2012) 07E702.
- [70] J. Jeong, D. Jang, D. Kim, D. Lee, S.K. Chung, Acoustic bubble-based drug manipulation: Carrying, releasing and penetrating for targeted drug delivery using an electromagnetically actuated microrobot, *Sens. Actuators, A* 306 (2020) 111973.
- [71] S. Yuan, Y. Wan, S. Song, RectMag3D: A Magnetic Actuation System for Steering Milli/Microrobots Based on Rectangular Electromagnetic Coils, *Appl. Sci.* 10 (8) (2020).
- [72] Y. Dai, S. Liang, Y. Chen, Y. Feng, D. Chen, B. Song, X. Bai, D. Zhang, L. Feng, F. Arai, Untethered Octopus-Inspired Millirobot Actuated by Regular Tetrahedron Arranged Magnetic Field, *Adv. Intell. Syst.* 2 (5) (2020) 1900148.
- [73] A. Azizi, C.C. Tremblay, K. Gagné, S. Martel, Using the fringe field of a clinical MRI scanner enables robotic navigation of tethered instruments in deeper vascular regions, *Science, Robotics* 4 (36) (2019) eaax7342.
- [74] A.W. Mahoney, J.J. Abbott, Five-degree-of-freedom manipulation of an untethered magnetic device in fluid using a single permanent magnet with application in stomach capsule endoscopy, *Int. J. Robot. Res.* 35 (1–3) (2015) 129–147.
- [75] H. Choi, S. Jeong, C. Lee, B.J. Park, S.Y. Ko, J.-O. Park, S.J.I.J.o.C. Park, Automation, Systems, Three-dimensional swimming tadpole mini-robot using three-axis Helmholtz coils, 12(3) (2014) 662–669.
- [76] A.M. Maier, C. Weig, P. Oswald, E. Frey, P. Fischer, T. Liedl, Magnetic Propulsion of Microswimmers with DNA-Based Flagellar Bundles, *Nano Lett.* 16 (2) (2016) 906–910.
- [77] Y. Ko, S. Na, Y. Lee, K. Cha, S.Y. Ko, J. Park, S. Park, A jellyfish-like swimming mini-robot actuated by an electromagnetic actuation system, *Smart Mater. Struct.* 21 (5) (2012) 057001.
- [78] S. Schuerle, S. Erni, M. Flink, B.E. Kratochvil, B.J. Nelson, Three-Dimensional Magnetic Manipulation of Micro- and Nanostructures for Applications in Life Sciences, *IEEE Trans. Magn.* 49 (1) (2013) 321–330.
- [79] J. Nam, W. Lee, E. Jung, G. Jang, Magnetic Navigation System Utilizing a Closed Magnetic Circuit to Maximize Magnetic Field and a Mapping Method to Precisely Control Magnetic Field in Real Time, *IEEE Trans. Ind. Electron.* 65 (7) (2018) 5673–5681.
- [80] O. Yasa, P. Erkoc, Y. Alapan, M. Sitti, Microalga-Powered Microswimmers toward Active Cargo Delivery, *Adv. Mater.* 30 (45) (2018) 1804130.
- [81] M. Dong, X. Wang, X.-Z. Chen, F. Mushtaq, S. Deng, C. Zhu, H. Torlakci, A. Terzopoulou, X.-H. Qin, X. Xiao, J. Puigmarti-Luis, H. Choi, A.P. Pêgo, Q.-D. Shen, B.J. Nelson, S. Pané, 3D-Printed Soft Magnetoelectric Microswimmers for Delivery and Differentiation of Neuron-Like Cells, *Adv. Funct. Mater.* 30 (17) (2020) 1910323.
- [82] V. Magdanz, S. Sanchez, O.G. Schmidt, Development of a Sperm-Flagella Driven Micro-Bio-Robot, *Adv. Mater.* 25 (45) (2013) 6581–6588.
- [83] X. Wang, J. Cai, L. Sun, S. Zhang, D. Gong, X. Li, S. Yue, L. Feng, D. Zhang, Facile Fabrication of Magnetic Microbots Based on Spirulina Templates for Targeted Delivery and Synergistic Chemo-Photothermal Therapy, *ACS Appl. Mater. Interfaces* 11 (5) (2019) 4745–4756.
- [84] P. Dhar, S. Narendren, S.S. Gaur, S. Sharma, A. Kumar, V. Katiyar, Self-propelled cellulose nanocrystal based catalytic nanomotors for targeted hyperthermia and pollutant remediation applications, *Int. J. Biol. Macromol.* 158 (2020) 1020–1036.
- [85] A.V. Singh, M.H. Dad Ansari, C.B. Dayan, J. Giltinan, S. Wang, Y. Yu, V. Kishore, P. Laux, A. Luch, M. Sitti, Multifunctional magnetic hairbot for untethered osteogenesis, ultrasound contrast imaging and drug delivery, *Biomaterials* 219 (2019) 119394.
- [86] R.C. Mundargi, M.G. Potroz, S. Park, H. Shirahama, J.H. Lee, J. Seo, N.-J. Cho, Natural Sunflower Pollen as a Drug Delivery Vehicle, *Small* 12 (9) (2016) 1167–1173.
- [87] R.C. Mundargi, M.G. Potroz, J.H. Park, J. Seo, J.H. Lee, N.-J. Cho, Extraction of sporopollenin exine capsules from sunflower pollen grains, *RSC Adv.* 6 (20) (2016) 16533–16539.
- [88] J. Li, X. Li, T. Luo, R. Wang, C. Liu, S. Chen, D. Li, J. Yue, S.-H. Cheng, D. Sun, Development of a magnetic microrobot for carrying and delivering targeted cells, *Science, Robotics* 3 (19) (2018) eaat8229.
- [89] S. Tottori, L. Zhang, F. Qiu, K.K. Krawczyk, A. Franco-Obregón, B.J. Nelson, Magnetic Helical Micromachines: Fabrication, Controlled Swimming, and Cargo Transport, *Adv. Mater.* 24 (6) (2012) 811–816.
- [90] H. Ceylan, I.C. Yasa, O. Yasa, A.F. Tabak, J. Giltinan, M. Sitti, 3D-Printed Biodegradable Microswimmer for Theranostic Cargo Delivery and Release, *ACS Nano* 13 (3) (2019) 3353–3362.
- [91] D.-I. Kim, H. Lee, S.-H. Kwon, H. Choi, S. Park, Magnetic nano-particles retrievable biodegradable hydrogel microrobot, *Sens. Actuators B* 289 (2019) 65–77.
- [92] M. Sun, X. Fan, X. Meng, J. Song, W. Chen, L. Sun, H. Xie, Magnetic biohybrid micromotors with high maneuverability for efficient drug loading and targeted drug delivery, *Nanoscale* 11 (39) (2019) 18382–18392.
- [93] J. Park, J.-Y. Kim, S. Pané, B.J. Nelson, H. Choi, Acoustically Mediated Controlled Drug Release and Targeted Therapy with Degradable 3D Porous Magnetic Microrobots, *Adv. Healthc. Mater.* 10 (2) (2021) 2001096.
- [94] P. Pouponneau, J.-C. Leroux, G. Soulez, L. Gaboury, S. Martel, Co-encapsulation of magnetic nanoparticles and doxorubicin into biodegradable microcarriers for deep tissue targeting by vascular MRI navigation, *Biomaterials* 32 (13) (2011) 3481–3486.
- [95] G. Chatzipiridis, O. Ergeneman, J. Pokki, F. Ullrich, S. Fusco, J.A. Ortega, K.M. Sivaraman, B.J. Nelson, S. Pané, Electroforming of Implantable Tubular Magnetic Microrobots for Wireless Ophthalmologic Applications, *Adv. Healthc. Mater.* 4 (2) (2015) 209–214.
- [96] F. Qiu, S. Fujita, R. Mhanna, L. Zhang, B.R. Simona, B.J. Nelson, Magnetic Helical Microswimmers Functionalized with Lipoplexes for Targeted Gene Delivery, *Adv. Funct. Mater.* 25 (11) (2015) 1666–1671.
- [97] I.C. Yasa, H. Ceylan, U. Bozuyuk, A.-M. Wild, M. Sitti, Elucidating the interaction dynamics between microswimmer body and immune system for medical microrobots, *Science, Robotics* 5 (43) (2020) eaaz3867.
- [98] S. Kim, S. Lee, J. Lee, B.J. Nelson, L. Zhang, H. Choi, Fabrication and Manipulation of Ciliary Microrobots with Non-reciprocal Magnetic Actuation, *Sci. Rep.* 6 (1) (2016) 30713.
- [99] S. Jeon, S. Kim, S. Ha, S. Lee, E. Kim, S.Y. Kim, S.H. Park, J.H. Jeon, S.W. Kim, C. Moon, B.J. Nelson, J.-Y. Kim, S.-W. Yu, H. Choi, Magnetically actuated microrobots as a platform for stem cell transplantation, *Science, Robotics* 4 (30) (2019) eaav4317.
- [100] L. Zhang, T. Petit, K.E. Peyer, B.J. Nelson, Targeted cargo delivery using a rotating nickel nanowire, *Nanomedicine: Nanotechnology, Biology and Medicine* 8 (7) (2012) 1074–1080.
- [101] S.K. Srivastava, M. Medina-Sánchez, B. Koch, O.G. Schmidt, Medibots: Dual-Action Biogenic Microdaggers for Single-Cell Surgery and Drug Release, *Adv. Mater.* 28 (5) (2016) 832–837.
- [102] T. Xu, J. Zhang, M. Salehzadeh, O. Onaizah, E. Diller, Millimeter-scale flexible robots with programmable three-dimensional magnetization and motions, *Science, Robotics* 4 (29) (2019) eaav4494.
- [103] Y. Alapan, A.C. Karacakol, S.N. Guzelhan, I. Isik, M. Sitti, Reprogrammable shape morphing of magnetic soft machines, *Science, Advances* 6 (38) (2020) eabc6414.
- [104] B.-W. Park, J. Zhuang, O. Yasa, M. Sitti, Multifunctional Bacteria-Driven Microswimmers for Targeted Active Drug Delivery, *ACS Nano* 11 (9) (2017) 8910–8923.
- [105] Z. Wu, B. Esteban-Fernández de Ávila, A. Martín, C. Christianson, W. Gao, S.K. Thamphiphatana, A. Escarpa, Q. He, L. Zhang, J. Wang, RBC micromotors carrying multiple cargos towards potential theranostic applications, *Nanoscale* 7 (32) (2015) 13680–13686.
- [106] H. Xu, M. Medina-Sánchez, O.G. Schmidt, Magnetic Micromotors for Multiple Motile Sperm Cells Capture, Transport, and Enzymatic Release, *Angew. Chem. Int. Ed.* 59 (35) (2020) 15029–15037.

- [107] C.C.J. Alcántara, S. Kim, S. Lee, B. Jang, P. Thakolkaran, J.-Y. Kim, H. Choi, B.J. Nelson, S. Pané, 3D Fabrication of Fully Iron Magnetic Microrobots, *Small* 15 (16) (2019) 1805006.
- [108] M.-J. Tang, W. Wang, Z.-L. Li, Z.-M. Liu, Z.-Y. Guo, H.-Y. Tian, Z. Liu, X.-J. Ju, R. Xie, L.-Y. Chu, Controllable Microfluidic Fabrication of Magnetic Hybrid Microswimmers with Hollow Helical Structures, *Ind. Eng. Chem. Res.* 57 (29) (2018) 9430–9438.
- [109] H. Gu, Q. Boehler, H. Cui, E. Secchi, G. Savorana, C. De Marco, S. Gervasoni, Q. Peyron, T.-Y. Huang, S. Pane, A.M. Hirt, D. Ahmed, B.J. Nelson, Magnetic cilia carpets with programmable metachronal waves, *Nat. Commun.* 11 (1) (2020) 2637.
- [110] S. Won, H. Je, S. Kim, J.J. Wie, Agile Underwater Swimming of Magnetic Polymeric Microrobots in Viscous Solutions, *Adv. Intell. Syst.* 4 (6) (2022) 2100269.
- [111] X. Yan, Q. Zhou, M. Vincent, Y. Deng, J. Yu, J. Xu, T. Xu, T. Tang, L. Bian, Y.-X.-J. Wang, K. Kostarelos, L. Zhang, Multifunctional biohybrid magnetite microrobots for imaging-guided therapy, *Science, Robotics* 2 (12) (2017) eaag1155.
- [112] X. Wang, C. Hu, L. Schurz, C. De Marco, X. Chen, S. Pané, B.J. Nelson, Surface-Chemistry-Mediated Control of Individual Magnetic Helical Microswimmers in a Swarm, *ACS Nano* 12 (6) (2018) 6210–6217.
- [113] H.C. Sun, P. Liao, T. Wei, L. Zhang, D. Sun, Magnetically Powered Biodegradable Microswimmers, *Micromachines* 11 (4) (2020).
- [114] B. Jang, E. Gutman, N. Stucki, B.F. Seitz, P.D. Wendel-García, T. Newton, J. Pokki, O. Ergeneman, S. Pané, Y. Or, B.J. Nelson, Undulatory Locomotion of Magnetic Multilink Nanoswimmers, *Nano Lett.* 15 (7) (2015) 4829–4833.
- [115] F. Mushtaq, H. Torlakcić, M. Hoop, B. Jang, F. Carlson, T. Grunow, N. Läubli, A. Ferreira, X.-Z. Chen, B.J. Nelson, S. Pané, Motile Piezoelectric Nanoneels for Targeted Drug Delivery, *Adv. Funct. Mater.* 29 (12) (2019) 1808135.
- [116] Y. Zhao, H. Xiong, Y. Li, W. Gao, C. Hua, J. Wu, C. Fan, X. Cai, Y. Zheng, Magnetically Actuated Reactive Oxygen Species Scavenging Nano-Robots for Targeted Treatment, *Adv. Intell. Syst.* 4 (7) (2022) 2200061.
- [117] M.M. Stanton, B.-W. Park, A. Miguel-López, X. Ma, M. Sitti, S. Sánchez, Biohybrid Microtube Swimmers Driven by Single Captured Bacteria, *Small* 13 (19) (2017) 1603679.
- [118] J. Liu, J. Li, G. Wang, W. Yang, J. Yang, Y. Liu, Bioinspired zeolitic imidazolate framework (ZIF-8) magnetic micromotors for highly efficient removal of organic pollutants from water, *J. Colloid Interface Sci.* 555 (2019) 234–244.
- [119] S. Zhu, W. Zheng, J. Wang, X. Fang, L. Zhang, F. Niu, Y. Wang, T. Luo, G. Liu, R. Yang, Interactive and synergistic behaviours of multiple heterogeneous microrobots, *Lab Chip* 22 (18) (2022) 3412–3423.
- [120] T. Li, J. Li, K.I. Morozov, Z. Wu, T. Xu, I. Rozen, A.M. Leshansky, L. Li, J. Wang, Highly Efficient Freestyle Magnetic Nanoswimmer, *Nano Lett.* 17 (8) (2017) 5092–5098.
- [121] K. Yoshida, H. Onoe, Functionalized core-shell hydrogel microsprings by anisotropic gelation with bevel-tip capillary, *Sci. Rep.* 7 (1) (2017) 45987.
- [122] J. Giltinan, P. Katsamba, W. Wang, E. Lauga, M. Sitti, Selectively controlled magnetic microrobots with opposing helices, *Appl. Phys. Lett.* 116 (13) (2020) 134101.
- [123] A. Ghosh, D. Paria, G. Rangarajan, A. Ghosh, Velocity Fluctuations in Helical Propulsion: How Small Can a Propeller Be, *J. Phys. Chem. Lett.* 5 (1) (2014) 62–68.
- [124] X. Yan, Q. Zhou, J. Yu, T. Xu, Y. Deng, T. Tang, Q. Feng, L. Bian, Y. Zhang, A. Ferreira, L. Zhang, Magnetite Nanostructured Porous Hollow Helical Microswimmers for Targeted Delivery, *Adv. Funct. Mater.* 25 (33) (2015) 5333–5342.
- [125] K.I. Morozov, A.M. Leshansky, Dynamics and polarization of superparamagnetic chiral nanomotors in a rotating magnetic field, *Nanoscale* 6 (20) (2014) 12142–12150.
- [126] C. Xin, L. Yang, J. Li, Y. Hu, Q. Jian, S. Fan, K. Hu, Z. Cai, H. Wu, D. Wang, D. Wu, J. Chu, Conical Hollow Microhelices with Superior Swimming Capabilities for Targeted Cargo Delivery, *Adv. Mater.* 31 (25) (2019) 1808226.
- [127] X.-Z. Chen, J.-H. Liu, M. Dong, L. Müller, G. Chatzipirpiridis, C. Hu, A. Terzopoulou, H. Torlakcić, X. Wang, F.J.M.H. Mushtaq, Magnetically driven piezoelectric soft microswimmers for neuron-like cell delivery and neuronal differentiation, 6(7) (2019) 1512–1516.
- [128] F. Zhao, W. Rong, D. Li, L. Wang, L. Sun, Four-dimensional design and programming of shape-memory magnetic helical micromachines, *Appl. Mater. Today* 27 (2022) 101422.
- [129] H. Xu, M. Medina-Sánchez, V. Magdanz, L. Schwarz, F. Hebenstreit, O.G. Schmidt, Sperm-Hybrid Micromotor for Targeted Drug Delivery, *ACS Nano* 12 (1) (2018) 327–337.
- [130] E. Diller, J. Zhuang, G. Zhan Lum, M.R. Edwards, M. Sitti, Continuously distributed magnetization profile for millimeter-scale elastomeric undulatory swimming, *Appl. Phys. Lett.* 104 (17) (2014) 174101.
- [131] F. Striggow, M. Medina-Sánchez, G.K. Auernhammer, V. Magdanz, B.M. Friedrich, O.G. Schmidt, Sperm-Driven Micromotors Moving in Oviduct Fluid and Viscoelastic Media, *Small* 16 (24) (2020) 2000213.
- [132] V. Magdanz, B. Koch, S. Sanchez, O.G. Schmidt, Sperm Dynamics in Tubular Confinement, *Small* 11 (7) (2015) 781–785.
- [133] T. Li, A. Zhang, G. Shao, M. Wei, B. Guo, G. Zhang, L. Li, W. Wang, Janus Micromer Surface Walkers Propelled by Oscillating Magnetic Fields, *Adv. Funct. Mater.* 28 (25) (2018) 1706066.
- [134] K. Yuan, V. de la Asunción-Nadal, B. Jurado-Sánchez, A. Escarpa, 2D Nanomaterials Wrapped Janus Micromotors with Built-in Multiengines for Bubble Magnetic, and Light Driven Propulsion, *Chem. Mater.* 32 (5) (2020) 1983–1992.
- [135] K. Villa, L. Krejčová, F. Novotný, Z. Heger, Z. Sofer, M. Pumera, Cooperative Multifunctional Self-Propelled Paramagnetic Microrobots with Chemical Handles for Cell Manipulation and Drug Delivery, *Adv. Funct. Mater.* 28 (43) (2018) 1804343.
- [136] J. Li, S. Thamphiwatana, W. Liu, B. Esteban-Fernández de Ávila, P. Angsantikul, E. Sandraz, J. Wang, T. Xu, F. Soto, V. Ramez, X. Wang, W. Gao, L. Zhang, J. Wang, Enteric Micromotor Can Selectively Position and Spontaneously Propel in the Gastrointestinal Tract, *ACS Nano* 10 (10) (2016) 9536–9542.
- [137] P. Liao, L. Xing, S. Zhang, D. Sun, Magnetically Driven Undulatory Microswimmers Integrating Multiple Rigid Segments, *Small* 15 (36) (2019) 1901197.
- [138] N. Hu, L. Wang, W. Zhai, M. Sun, H. Xie, Z. Wu, Q. He, Magnetically Actuated Rolling of Star-Shaped Hydrogel Microswimmer, *Macromol. Chem. Phys.* 219 (5) (2018) 1700540.
- [139] W.H. Ko, Trends and frontiers of MEMS, *Sens. Actuators, A* 136 (1) (2007) 62–67.
- [140] Y. Zhang, K. Yan, F. Ji, L. Zhang, Enhanced Removal of Toxic Heavy Metals Using Swarming Biohybrid Adsorbents, *Adv. Funct. Mater.* 28 (52) (2018) 1806340.
- [141] Y. Zhang, L. Zhang, L. Yang, C.I. Vong, K.F. Chan, W.K.K. Wu, T.N.Y. Kwong, N. W.S. Lo, M. Ip, S.H. Wong, J.J.Y. Sung, P.W.Y. Chiu, L. Zhang, Real-time tracking of fluorescent magnetic spore-based microrobots for remote detection of em; diff; em; toxins, *Science, Advances* 5 (1) (2019) eaau9650.
- [142] W. Gao, X. Feng, A. Pei, C.R. Kane, R. Tam, C. Hennessy, J. Wang, Bioinspired Helical Microswimmers Based on Vascular Plants, *Nano Lett.* 14 (1) (2014) 305–310.
- [143] S. Kim, F. Qiu, S. Kim, A. Ghanbari, C. Moon, L. Zhang, B.J. Nelson, H. Choi, Fabrication and Characterization of Magnetic Microrobots for Three-Dimensional Cell Culture and Targeted Transportation, *Adv. Mater.* 25 (41) (2013) 5863–5868.
- [144] X. Wang, X.-H. Qin, C. Hu, A. Terzopoulou, X.-Z. Chen, T.-Y. Huang, K. Maniura-Weber, S. Pané, B.J. Nelson, 3D Printed Enzymatically Biodegradable Soft Helical Microswimmers, *Adv. Funct. Mater.* 28 (45) (2018) 1804107.
- [145] P. Cabanach, A. Pena-Francesch, D. Sheehan, U. Bozuyuk, O. Yasa, S. Borros, M. Sitti, Zwitterionic 3D-Printed Non-Immunogenic Stealth Microrobots, *Adv. Mater.* 32 (42) (2020) 2003013.
- [146] C.C.J. Alcántara, F.C. Landers, S. Kim, C. De Marco, D. Ahmed, B.J. Nelson, S. Pané, Mechanically interlocked 3D multi-material micromachines, *Nat. Commun.* 11 (1) (2020) 5957.
- [147] W. Gao, R. Dong, S. Thamphiwatana, J. Li, W. Gao, L. Zhang, J. Wang, Artificial Micromotors in the Mouse's Stomach: A Step toward In Vivo Use of Synthetic Motors, *ACS Nano* 9 (1) (2015) 117–123.
- [148] J. Li, S. Sattayasamitsathit, R. Dong, W. Gao, R. Tam, X. Feng, S. Ai, J. Wang, Template electrosynthesis of tailored-made helical nanoswimmers, *Nanoscale* 6 (16) (2014) 9415–9420.
- [149] T. Li, J. Li, H. Zhang, X. Chang, W. Song, Y. Hu, G. Shao, E. Sandraz, G. Zhang, L. Li, J. Wang, Magnetically Propelled Fish-Like Nanoswimmers, *Small* 12 (44) (2016) 6098–6105.
- [150] F. Mushtaq, A. Asani, M. Hoop, X.-Z. Chen, D. Ahmed, B.J. Nelson, S. Pané, Highly Efficient Coaxial TiO₂-PtPd Tubular Nanomachines for Photocatalytic Water Purification with Multiple Locomotion Strategies, *Adv. Funct. Mater.* 26 (38) (2016) 6995–7002.
- [151] J. Li, P. Angsantikul, W. Liu, B. Esteban-Fernández de Ávila, X. Chang, E. Sandraz, Y. Liang, S. Zhu, Y. Zhang, C. Chen, W. Gao, L. Zhang, J. Wang, Biomimetic Platelet-Camouflaged Nanorobots for Binding and Isolation of Biological Threats, *Adv. Mater.* 30 (2) (2018) 1704800.
- [152] J. Wu, B. Jang, Y. Harduf, Z. Chapnik, Ö.B. Avci, X. Chen, J. Puigmartí-Luis, O. Ergeneman, B.J. Nelson, Y. Or, S. Pané, Helical Klinotactic Locomotion of Two-Link Nanoswimmers with Dual-Function Drug-Loaded Soft Polysaccharide Hinges, *Adv. Sci.* 8 (8) (2021) 2004458.
- [153] Z. Wu, J. Troll, H.-H. Jeong, Q. Wei, M. Stang, F. Ziemssen, Z. Wang, M. Dong, S. Schnichels, T. Qiu, P. Fischer, A swarm of slippery micropropellers penetrates the vitreous body of the eye, *Science, Advances* 4 (11) (2018) eaat4388.
- [154] D. Walker, B.T. Käsdorf, H.-H. Jeong, O. Lieleg, P. Fischer, Enzymatically active biomimetic micropropellers for the penetration of mucin gels, *Sci. Adv.* 1 (11) (2015) e1500501.
- [155] D. Schamel, A.G. Mark, J.G. Gibbs, C. Miksch, K.I. Morozov, A.M. Leshansky, P. Fischer, Nanopropellers and Their Actuation in Complex Viscoelastic Media, *ACS Nano* 8 (9) (2014) 8794–8801.
- [156] P.L. Venugopalan, S. Jain, S. Shivashankar, A. Ghosh, Single coating of zinc ferrite renders magnetic nanomotors therapeutic and stable against agglomeration, *Nanoscale* 10 (5) (2018) 2327–2332.
- [157] X.-Z. Chen, M. Hoop, N. Shamsudhin, T. Huang, B. Özkal, Q. Li, E. Siringil, F. Mushtaq, L. Di Tizio, B.J. Nelson, S. Pané, Hybrid Magnetoelectric Nanowires for Nanorobotic Applications: Fabrication, Magnetoelectric Coupling, and Magnetically Assisted In Vitro Targeted Drug Delivery, *Adv. Mater.* 29 (8) (2017) 1605458.
- [158] Y. Yin, T. Qiu, L. Ma, X. Lang, Y. Zhang, G. Huang, Y. Mei, O.G. Schmidt, Exploring Rolled-up Au–Ag Bimetallic Microtubes for Surface-Enhanced Raman Scattering Sensor, *J. Phys. Chem. C* 116 (48) (2012) 25504–25508.
- [159] L. Zhang, J.J. Abbott, L. Dong, K.E. Peyer, B.E. Kratochvil, H. Zhang, C. Bergeles, B.J. Nelson, Characterizing the Swimming Properties of Artificial Bacterial Flagella, *Nano Lett.* 9 (10) (2009) 3663–3667.

- [160] L. Zhang, J.J. Abbott, L. Dong, B.E. Kratochvil, D. Bell, B.J. Nelson, Artificial bacterial flagella: Fabrication and magnetic control, *Appl. Phys. Lett.* 94 (6) (2009) 064107.
- [161] W. Xi, A.A. Solovev, A.N. Ananth, D.H. Gracias, S. Sanchez, O.G.J.N. Schmidt, Rolled-up magnetic microdrillers: towards remotely controlled minimally invasive surgery, 5(4) (2013) 1294–1297.
- [162] A. Sitt, J. Soukupova, D. Miller, D. Verdi, R. Zboril, H. Hess, J. Lahann, Microscale Rockets and Picoliter Containers Engineered from Electrospun Polymeric Microtubes, *Small* 12 (11) (2016) 1432–1439.
- [163] D. Wang, G. Zhao, C. Chen, H. Zhang, R. Duan, D. Zhang, M. Li, B. Dong, One-Step Fabrication of Dual Optically/Magnetically Modulated Walnut-like Micromotor, *Langmuir* 35 (7) (2019) 2801–2807.
- [164] Y. Su, T. Qiu, W. Song, X. Han, M. Sun, Z. Wang, H. Xie, M. Dong, M. Chen, Melt Electrospinning Writing of Magnetic Microrobots, *Adv. Sci.* 8 (3) (2021) 2003177.
- [165] I.S.M. Khalil, A.F. Tabak, A. Hosney, A. Mohamed, A. Klingner, M. Ghoneima, M. Sitti, Sperm-shaped magnetic microrobots: Fabrication using electrospinning, modeling, and characterization, *IEEE International Conference on Robotics and Automation (ICRA) 2016* (2016) 1939–1944.
- [166] R. Mhanma, F. Qiu, L. Zhang, Y. Ding, K. Sugihara, M. Zenobi-Wong, B.J. Nelson, Artificial Bacterial Flagella for Remote-Controlled Targeted Single-Cell Drug Delivery, *Small* 10 (10) (2014) 1953–1957.
- [167] H.W. Huang, F.E. Uslu, P. Katsamba, E. Lauga, M.S. Sakar, B.J. Nelson, Adaptive locomotion of artificial microswimmers, *Science, Advances* 5 (1) (2019) eaau1532.
- [168] V.M. Kadri, C. Bussi, A.W. Holle, K. Son, H. Kwon, G. Schütz, M.G. Gutierrez, P. Fischer, Biocompatible Magnetic Micro- and Nanodevices: Fabrication of FePt Nanopropellers and Cell Transfection, *Adv. Mater.* 32 (25) (2020) 2001114.
- [169] X. Song, Z. Chen, X. Zhang, J. Xiong, T. Jiang, Z. Wang, X. Geng, U.K. Cheang, Magnetic tri-bead microrobot assisted near-infrared triggered combined photothermal and chemotherapy of cancer cells, *Sci. Rep.* 11 (1) (2021) 7907.
- [170] V.D. Nguyen, H.-K. Min, H.Y. Kim, J. Han, Y.H. Choi, C.-S. Kim, J.-O. Park, E. Choi, Primary Macrophage-Based Microrobots: An Effective Tumor Therapy In Vivo by Dual-Targeting Function and Near-Infrared-Triggered Drug Release, *ACS Nano* 15 (5) (2021) 8492–8506.
- [171] M. Xie, W. Zhang, C. Fan, C. Wu, Q. Feng, J. Wu, Y. Li, R. Gao, Z. Li, Q. Wang, Y. Cheng, B. He, Bioinspired Soft Microrobots with Precise Magneto-Collective Control for Microvascular Thrombolysis, *Adv. Mater.* 32 (26) (2020) 2000366.
- [172] T. Wei, J. Liu, D. Li, S. Chen, Y. Zhang, J. Li, L. Fan, Z. Guan, C.-M. Lo, L. Wang, K. Man, D. Sun, Development of Magnet-Driven and Image-Guided Degradable Microrobots for the Precise Delivery of Engineered Stem Cells for Cancer Therapy, *Small* 16 (41) (2020) 1906908.
- [173] M. Nair, R. Guduru, P. Liang, J. Hong, V. Sagar, S. Khizroev, Externally controlled on-demand release of anti-HIV drug using magneto-electric nanoparticles as carriers, *Nat. Commun.* 4 (1) (2013) 1707.
- [174] W. Chen, M. Sun, X. Fan, H. Xie, Magnetic/pH-sensitive double-layer microrobots for drug delivery and sustained release, *Appl. Mater. Today* 19 (2020) 100583.
- [175] X. Yan, J. Xu, Q. Zhou, D. Jin, C.I. Vong, Q. Feng, D.H.L. Ng, L. Bian, L. Zhang, Molecular cargo delivery using multicellular magnetic microswimmers, *Applied. Mater. Today* 15 (2019) 242–251.
- [176] U. Bozuyuk, O. Yasa, I.C. Yasa, H. Ceylan, S. Kizilel, M. Sitti, Light-Triggered Drug Release from 3D-Printed Magnetic Chitosan Microswimmers, *ACS Nano* 12 (9) (2018) 9617–9625.
- [177] K.-W. Gyak, S. Jeon, L. Ha, S. Kim, J.-Y. Kim, K.-S. Lee, H. Choi, D.-P. Kim, Magnetically Actuated SiCN-Based Ceramic Microrobot for Guided Cell Delivery, *Adv. Healthc. Mater.* 8 (21) (2019) 1900739.
- [178] P. Zhang, G. Wu, C. Zhao, L. Zhou, X. Wang, S. Wei, Magnetic stomatocyte-like nanomotor as photosensitizer carrier for photodynamic therapy based cancer treatment, *Colloids Surf. B Biointerfaces* 194 (2020) 111204.
- [179] H. Lee, D.-I. Kim, S.-H. Kwon, S. Park, Magnetically Actuated Drug Delivery Helical Microrobot with Magnetic Nanoparticle Retrieval Ability, *ACS Appl. Mater. Interfaces* 13 (17) (2021) 19633–19647.
- [180] W. Chen, Y. Wen, X. Fan, M. Sun, C. Tian, M. Yang, H. Xie, Magnetically actuated intelligent hydrogel-based child-parent microrobots for targeted drug delivery, *J. Mater. Chem. B* 9 (4) (2021) 1030–1039.
- [181] S. Jeong, H. Choi, G. Go, C. Lee, K.S. Lim, D.S. Sim, M.H. Jeong, S.Y. Ko, J.-O. Park, S. Park, Penetration of an artificial arterial thromboembolism in a live animal using an intravascular therapeutic microrobot system, *Med. Eng. Phys.* 38 (4) (2016) 403–410.
- [182] G. Go, A. Yoo, K.T. Nguyen, M. Nan, B.A. Darmawan, S. Zheng, B. Kang, C.-S. Kim, D. Bang, S. Lee, K.-P. Kim, S.S. Kang, K.M. Shim, S.E. Kim, S. Bang, D.-H. Kim, J.-O. Park, E. Choi, Multifunctional microrobot with real-time visualization and magnetic resonance imaging for chemoembolization therapy of liver cancer, *Science Advances* 8(46) eabq8545.
- [183] Q. Jin, Y. Yang, J.A. Jackson, C. Yoon, D.H. Gracias, Untethered Single Cell Grippers for Active Biopsy, *Nano Lett.* 20 (7) (2020) 5383–5390.
- [184] A. Ghosh, C. Yoon, F. Ongaro, S. Scheggi, F.M. Selaru, S. Misra, D.H. Gracias, Stimuli-Responsive Soft Untethered Grippers for Drug Delivery and Robotic Surgery, 3(7) (2017).
- [185] S.J. Kim, G.H. Jang, S.M. Jeon, J.K. Nam, A crawling and drilling microrobot driven by an external oscillating or precessional magnetic field in tubular environments, *J. Appl. Phys.* 117 (17) (2015) 17A703.
- [186] H. Yang, Z. Yang, D. Jin, L. Su, K.F. Chan, K.K.L. Chong, C.P. Pang, L. Zhang, Magnetic Micro-Driller System for Nasolacrimal Duct Recanalization, *IEEE Rob. Autom. Lett.* 7 (3) (2022) 7367–7374.
- [187] K.T. Nguyen, S.J. Kim, H.K. Min, M.C. Hoang, G. Go, B. Kang, J. Kim, E. Choi, A. Hong, J.O. Park, C.S. Kim, Guide-Wired Helical Microrobot for Percutaneous Revascularization in Chronic Total Occlusion in-Vivo Validation, *IEEE Trans. Biomed. Eng.* 68 (8) (2021) 2490–2498.
- [188] L. Feng, M. Hagiwara, A. Ichikawa, F. Arai, On-Chip Enucleation of Bovine Oocytes using Microrobot-Assisted Flow-Speed Control, *Micromachines* 4 (2) (2013).
- [189] Z. Lin, X. Fan, M. Sun, C. Gao, Q. He, H. Xie, Magnetically Actuated Peanut Colloid Motors for Cell Manipulation and Patterning, *ACS Nano* 12 (3) (2018) 2539–2545.
- [190] L. Schwarz, D.D. Karnaushenko, F. Hebenstreit, R. Naumann, O.G. Schmidt, M. Medina-Sánchez, A Rotating Spiral Micromotor for Noninvasive Zygote Transfer, *Adv. Sci.* 7 (18) (2020) 2000843.
- [191] D. Vilela, J. Parmar, Y. Zeng, Y. Zhao, S. Sánchez, Graphene-Based Microbots for Toxic Heavy Metal Removal and Recovery from Water, *Nano Lett.* 16 (4) (2016) 2860–2866.
- [192] F. Mushtaq, M. Guerrero, M.S. Sakar, M. Hoop, A.M. Lindo, J. Sort, X. Chen, B.J. Nelson, E. Pellicer, S.J.J.o.M.C.A. Pané, Magnetically driven Bi₂O₃/BiOCl-based hybrid microrobots for photocatalytic water remediation, 3(47) (2015) 23670–23676.
- [193] J. García-Torres, A. Serrà, P. Tierno, X. Alcobé, E. Vallés, Magnetic Propulsion of Recyclable Catalytic Nanocleaners for Pollutant Degradation, *ACS Appl. Mater. Interfaces* 9 (28) (2017) 23859–23868.
- [194] X. Li, Y.-M. Sun, Z.-Y. Zhang, N.-X. Feng, H. Song, Y.-L. Liu, L. Hai, J.-M. Cao, G.P. Wang, Visible light-driven multi-motion modes CNC/TiO₂ nanomotors for highly efficient degradation of emerging contaminants, *Carbon* 155 (2019) 195–203.
- [195] C.C. Mayorga-Martinez, J. Vyskočil, F. Novotný, P. Bednar, D. Ružek, O. Alduahish, M. Pumera, Collective behavior of magnetic microrobots through immuno-sandwich assay: On-the-fly COVID-19 sensing, *Appl. Mater. Today* 26 (2022) 101337.
- [196] Y. Wang, X. Liu, C. Chen, Y. Chen, Y. Li, H. Ye, B. Wang, H. Chen, J. Guo, X. Ma, Magnetic Nanorobots as Maneuverable Immunoassay Probes for Automated and Efficient Enzyme Linked Immunosorbent Assay, *ACS Nano* 16 (1) (2022) 180–191.
- [197] S. Tasoglu, E. Diller, S. Guven, M. Sitti, U. Demirci, Untethered micro-robotic coding of three-dimensional material composition, *Nat. Commun.* 5 (1) (2014) 3124.
- [198] O. Youssefi, E. Diller, Dry surface micromanipulation using an untethered magnetic microrobot, *Advances in Motion Sensing and Control for Robotic Applications*, Springer, 2019, pp. 75–91.
- [199] T. Yang, A. Tomaka, T.O. Tasci, K.B. Neeves, N. Wu, D.W.M. Marr, Microwheels on microroads: Enhanced translation on topographic surfaces, *Science, Robotics* 4 (32) (2019) eaaw9525.
- [200] M. Hagiwara, T. Kawahara, Y. Yamanishi, T. Masuda, L. Feng, F.J.L.o.A.C. Arai, On-chip magnetically actuated robot with ultrasonic vibration for single cell manipulations, 11(12) (2011) 2049–2054.
- [201] Q. Wang, J. Yu, K. Yuan, L. Yang, D. Jin, L. Zhang, Disassembly and spreading of magnetic nanoparticle clusters on uneven surfaces, *Appl. Mater. Today* 18 (2020) 100489.
- [202] H. Xie, M. Sun, X. Fan, Z. Lin, W. Chen, L. Wang, L. Dong, Q. He, Reconfigurable magnetic microrobot swarm: Multimode transformation, locomotion, and manipulation, *Science, Robotics* 4 (28) (2019) eaav8006.
- [203] X. Ma, L. Wang, P. Wang, Z. Liu, J. Hao, J. Wu, G. Chu, M. Huang, L.O. Mair, C. Huang, T. Xu, T. Ying, X. Tang, Y. Chen, X. Cai, Y. Zheng, An electromagnetically actuated magneto-nanozyme mediated synergistic therapy for destruction and eradication of biofilm, *Chem. Eng. J.* 431 (2022) 133971.
- [204] J. Rahmer, C. Stehning, B. Gleich, Spatially selective remote magnetic actuation of identical helical micromachines, *Science, Robotics* 2 (3) (2017) eaal2845.